Atmospheric Chemistry and Physics Discussions

ACPD

10, 4823–4885, 2010

Atmospheric Brown Clouds in the Himalayas: first two years of observations

P. Bonasoni et al.

Title Page

Abstract	Introduction
Conclusions	References
Tables	Figures

| ◄◄ | ►► |
| ◄ | ► |

| Back | Close |

Full Screen / Esc

Printer-friendly Version

Interactive Discussion

Atmospheric Brown Clouds in the Himalayas: first two years of continuous observations at the Nepal-Climate Observatory at Pyramid (5079 m)

P. Bonasoni[1,9], P. Laj[2], A. Marinoni[1], M. Sprenger[3], F. Angelini[1], J. Arduini[4], U. Bonafè[1], F. Calzolari[1], T. Colombo[5], S. Decesari[1], C. Di Biagio[6], A. G. di Sarra[6], F. Evangelisti[1], R. Duchi[1], M. C. Facchini[1], S. Fuzzi[1], G. P. Gobbi[1], M. Maione[4], A. Panday[7], F. Roccato[1], K. Sellegri[8], H. Venzac[2], G. P. Verza[9], P. Villani[2], E. Vuillermoz[9], and P. Cristofanelli[1]

[1]CNR – Institute for Atmospheric Sciences and Climate, Bologna, Italy

Atmospheric Brown Clouds in the Himalayas: first two years of observations

P. Bonasoni et al.

[2]Laboratoire de Glaciologie et Géophysique de l'Environnement, Université Grenoble 1 – CNRS, Grenoble, France

[3]ETHZ – Swiss Federal Institute of Technology, Zurich, Switzerland

[4]Urbino University, Chemistry Institute, Urbino, Italy

[5]CNMCA – Climate Department, Pratica di Mare, Roma, Italy

[6]ENEA, ACS-CLIM-OSS, Roma, Italy

[7]Department of Environmental Sciences, University of Virginia, Charlottesville, VA, USA

[8]Laboratoire de Météorologie Physique, CNRS – Université Blaise Pascal, Aubière, France

[9]Ev-K$_2$-CNR Committee, Bergamo, Italy

Correspondence to: P. Bonasoni (p.bonasoni@isac.cnr.it)

Title Page

Abstract	Introduction
Conclusions	References
Tables	Figures

|◄ | ►|

◄ | ►

| Back | Close |

Full Screen / Esc

Printer-friendly Version

Interactive Discussion

Abstract

South Asia is strongly influenced by the so-called Atmospheric Brown Cloud (ABC), a wide polluted layer extending from the Indian Ocean to the Himalayas during the winter and pre-monsoon seasons (November to April). This thick, grey-brown haze blanket substantially interacts with the incoming solar radiation, causing a cooling of the Earth's surface and a warming of the atmosphere, thus influencing the monsoon system and climate. In this area, the Himalayan region, particularly sensitive to climate change, offers a unique opportunity to detect global change processes and to analyse the influence of anthropogenic pollution on background atmospheric conditions through continuous monitoring activities.

This paper provides a detailed description of the atmospheric conditions character-izing the high Himalayas, thanks to continuous observations begun in March 2006 at the Nepal Climate Observatory – Pyramid (NCO-P) located at 5079 m a.s.l. on the southern foothills of Mt. Everest, in the framework of ABC-UNEP and SHARE-Ev-K^2-CNR projects. Besides giving an overview of the measurement site and experimental activities, the work presents an in-depth characterization of meteorological conditions and air-mass circulation at NCO-P during the first two years of activity (March 2006–February 2008). The mean values of atmospheric pressure, temperature and wind speed recorded at the site were: 551 hPa, $-3.0\,^\circ$C, 4.7 m s^{-1}, respectively. The highest seasonal values of temperature ($1.7\,^\circ$C) and relative humidity (94%) were registered during the monsoon season, which was also characterized by thick clouds present in about 80% of the afternoon hours and by a frequency of cloud-free sky less than 10%. The lowest temperature and relative humidity values were registered during winter, $-6.3\,^\circ$C and 22%, respectively, the season being characterised by mainly cloud-free sky conditions and rare thick clouds. The summer monsoon influenced the rain pre-cipitation (seasonal mean 237 mm), while wind was dominated by flows from the bot-tom of the valley (S-SW) and upper mountain (N-NE). In relation to seasonal weather conditions, the time series variability of black carbon and dust particles (optical active

aerosols) and ozone (regional greenhouse gas) were analysed, as they are significant constituents of the Atmospheric Brown Cloud and strongly influence the atmospheric radiative forcing. The highest seasonal values of black carbon (BC), ozone (O_3) and dust particles were observed during the pre-monsoon season (316.9 ng m^{-3},

5   60.9 ppbv, 0.37 cm^{-3}, respectively), while the lowest concentrations occurred during the monsoon for BC and O_3 (49.6 ng m^{-3} and 33.6 ppbv, respectively) and post-monsoon for dust particles (0.07 cm^{-3}). The seasonal cycles of these compounds are influenced both by the local mountain wind system and by the three principal large-scale circulation regimes: Westerly, South-Westerly and Regional, as shown by the

10   analysis of in-situ meteorological parameters and 5-day LAGRANTO back-trajectories. In particular, the analysis of data representative of synoptic-scale circulation showed that the highest median values (O_3: 68 ppbv, BC: 124 ng m^{-3}, dust particles: 0.44 cm^{-3}, respectively) were related with air-masses from polluted and arid regions in the Indian subcontinent, as well as the Arabian Peninsula and Persian Gulf. Furthermore, it was

15   documented that in 90% of pre-monsoon days the Khumbu valley represents a "direct channel" able to transport polluted air-masses from the Asian Brown Cloud up to NCO-P and to higher altitudes. On such days the average day-time BC concentration (625 ng m^{-3}) was at least double that recorded on the remaining days, even if during some pollution hot spots BC daily values increased up to 1000 ng m^{-3}.

20   In this study, two years of Himalayan observation activities carried out at NCO-P, in conjunction with model circulation analyses, provide some of the first evidence that polluted air-masses linked to the Atmospheric Brown Cloud can reach the high Himalayas, in particular during the pre-monsoon season, influencing the pristine atmospheric composition.

25   **1   Introduction**

During recent years, field experiments, in-situ observations and satellite monitoring have pointed to the existence of so-called "Brown Clouds", i.e. wide polluted

tropospheric layers characterised by anthropogenic aerosol optical depth (AOD) greater than 0.3 and absorbing AOD greater than 0.03 (Ramanathan et al., 2007, and references therein). Due to the large amount of gases and aerosol particles, including black carbon, these brown clouds have strong impacts on the air quality, visibility and energy budget of the troposphere. In the past decade, scientific research has been conducted over the Indo-Asia-Pacific region, where an extensive observation system has been developed within the INDOEX project (Ramanathan and Crutzen, 2003). Such observations have served to better investigate the so-called "Asian Brown Cloud", a large brown cloud extending from the Indian Ocean to the Himalayan range, attaining a vertical thickness of about 3 km (Ramanathan et al., 2007) during the dry season (especially from November to March), and affecting some of the most populous Asian regions, currently home to a population of more than 2 billion. For the purpose of improving knowledge about the "Brown Cloud" phenomenon and its influence on regional and global climate, air quality, public health and food security, the United Nations Environment Programme (UNEP) established the "Atmospheric Brown Cloud" (ABC) project (http://www.rrcap.unep.org/abc/). The research activities performed within ABC and previous projects (i.e. INDOEX, ACE-Asia, see Ramanathan and Crutzen, 2003; Huebert et al., 2003) have suggested that anthropogenic absorbing aerosols in the Atmospheric Brown Cloud warm the lower atmosphere just as much as greenhouse gases do (Ramanathan et al., 2007), leading to a major redistribution of solar radiation in the troposphere by dimming solar energy at the surface and enhancing the atmospheric heating rate. The Asian Brown Cloud is thus capable of producing a strong variation of the hydrological cycle associated with the South Asian monsoon. In fact, besides exerting a large south-north heating gradient between the equatorial Indian Ocean and Arabian Sea, the absorbing aerosols (black carbon and dust) within the Atmospheric Brown Cloud may also affect the Indian monsoon through the "Elevated Heat-pump" effect (Lau et al., 2006). Finally, the presence of large amounts of aerosol particles strongly influence the lifetime and microphysical properties of clouds, thus further influencing the regional water vapour cycle (Rosenfeld et al., 2008). Alongside

Atmospheric Brown Clouds in the Himalayas: first two years of observations

P. Bonasoni et al.

the aerosol particles emitted by fossil fuel and biomass burning (nitrate, sulphate, organic matter and black carbon), large amounts of gaseous pollutants (ozone, organic trace gases) have also been observed in the Atmospheric Brown Cloud (Ramanathan et al., 2008). Tropospheric ozone (O_3), in addition to being a harmful pollutant, also is
5 a strong greenhouse gas, and significant increases in its concentration can impact the regional radiative equilibrium of the troposphere (e.g. Ohara et al., 2007), further enhancing the atmospheric heating rate of absorbing aerosols. Although the ABC project activities have already allowed an improved understanding of the role of the Atmospheric Brown Cloud in affecting air-quality and climate on both the regional and global
10 scales, a gap in knowledge still exists concerning the characterization of the Asian Brown Cloud and its effects over the high Himalayas. In fact, even if the monitoring of atmospheric composition at high altitudes is recognised as playing an important role in climate change studies (e.g. by early detection of composition change, as well as by investigating the variability and seasonality of atmospheric compounds and the pos-
15 sible influence of hot-spot pollution), to date only sparse experimental work has been performed in this high-altitude region (Ramanthan et al., 2008; Shresta et al., 2000; Hindman et al., 2002; Carrico et al., 2003). It should be borne in mind that, while high mountain areas are generally considered to be "clean" regions, they can be strongly impacted by anthropogenic pollution (e.g. Henne et al., 2004; Cristofanelli et al., 2009).
20 The current issue aims to foster a better understanding of the characteristics of atmospheric conditions in the Himalayas, the world highest mountain region, which is located between China and India, two of the most rapidly developing areas in the world, and primary sources of anthropogenic pollution. A few previous investigations have already suggested that the southern Himalayas can be affected by significant amounts
25 of pollution uplifted by the typical valley circulations, or advected by regional and long-range transport events (e.g. Hindman et al., 2002; Hedge et al., 2007; Bonasoni et al., 2008). In particular, the thermal valley circulation can represent a preferred channel for the transport of polluted air-masses up to altitudes of 5000 m a.s.l., where the interaction between clean "upper" tropospheric air and more polluted boundary layer air rising

along the valley leads to very frequent new particle formation events (Venzac et al., 2008). Given their influence on the mountain ecosystem and tropospheric background conditions, and their role in the radiative equilibrium of the atmosphere and Earth's surface, the determination of absorbing aerosol and trace gas concentrations, together

5 with the investigation of processes influencing their variability, represent urgent tasks for the Himalayan region. The continuous monitoring of atmospheric composition in this area is crucial for evaluating the Asian background conditions of the free troposphere, and for quantifying the region's pollution levels.For the above reasons, in the framework of ABC-UNEP and SHARE (Station at High Altitude for Environmental research) – Ev-

10 K^2-CNR projects, the Nepal Climate Observatory – Pyramid (NCO-P) was installed in the high Khumbu valley (Nepal) at 5079 m a.s.l., in 2006 (Bonasoni et al., 2008). In particular, this research station was designed to perform continuous measurements of surface ozone, and to study the physical (mass and number size distribution), optical (absorption and scattering coefficients) and chemical (organic and inorganic, soluble

15 and insoluble) properties of aerosol. Climate-altering halocarbon concentrations are also measured weekly at NCO-P, while aerosol sun-photometry studies are carried out as part of the AERONET (AErosol RObotic NETwork) program (Gobbi et al., 2010).

Within the special issue "Atmospheric Brown Cloud in the Himalayas", the objective of this paper, is to evaluate the influence of the Asian Brown Cloud on the Himalayan

20 atmosphere composition. To this end and to investigate the possible role played by this Brown Cloud in affecting some of the climate-driving processes, the monitoring activities undertaken at NCO-P since March 2006 are presented and discussed. Instrumentation, technical set-up and analysis methodologies are initially illustrated, together with the description of synoptic and mesoscale models applied to depict air-mass circulation

25 culation at the measurement site. With the aim of providing basic information useful for other research activities conducted at NCO-P and presented in detail in the companion papers, the meteorological conditions at the station during the first two years of activity (March 2006–February 2008) are presented, identifying the seasonal transitions as a function of local weather regime and discussing the local and large-scale

⏮ | ⏭

◀ | ▶

Back | Close

Full Screen / Esc

air-mass circulation that characterised the measurement site. The variability of optically active aerosol, i.e. black carbon (BC) and coarse particles (with Dp>1 µm, here considered as a proxy of dust aerosol) and regional greenhouse gases, i.e. O_3, is also investigated for monsoon and non-monsoon seasons. In particular, for the purpose of
5   evaluating the influence of the Atmospheric Brown Cloud on the atmospheric composition in the South Himalayas, the BC, dust and O_3 behaviours were investigated as a function of different local/regional and synoptic circulation regimes observed during the pre-monsoon seasons. This permitted the identification and evaluation of the principal transport processes bringing high pollutant concentrations to this measurement site,
10 representative of the conditions of the South Himalayas troposphere.

2   Measurements and methodologies

2.1   Measurement site

The Nepal Climate Observatory – Pyramid (NCO-P, 27.95 N, 86.82 E) is located at 5079 m a.s.l. in Sagarmatha National Park, in the eastern Nepal Himalaya, near the
15 base camp area of Mt. Everest (Fig. 1). NCO-P is sited at the confluence of the secondary Lobuche valley (oriented NNW-SSE) and the main Khumbu valley (oriented NE-SW), a tributary of the Dudh Koshi valley, a major Ganges tributary. Forests exist only in areas of the valley below 4 km a.s.l., while the landscape around the measurement site is mostly rocky with patches of musk. The area is subject to short-lived snow cover
20 periods, especially during the cold months and summer monsoon. NCO-P is located away from important anthropogenic sources of pollutants, and only small villages are present along the valley: Lobuche, Pheriche, Tyangboche, Namche Bazar (the biggest village with about 800 inhabitants), Phakding and Lukla (Fig. 1). The closest major urban area is Kathmandu (1 081 845 inhabitants; 2001 census), situated in the valley of
25 the same name (estimated population of the valley in 2009 was ∼3 million). The city, located about 200 km South-West of the measurement site and more than 3.5 km lower

down, is characterised by high atmospheric pollution and poor air quality (Shrestha and Malla, 1996; Pudasainee et al., 2006; Panday and Prinn, 2009).The Observatory stands at the top of a hill, 200 m from the Pyramid International Laboratory, a multi-disciplinary high altitude research centre founded by the Ev-K^2-CNR Committee and the Nepal Academy of Science and Technology in 1990 (Baudo et al., 2007). NCO-P was set up during January and February 2006, and the observation program was launched at the end of February 2006 (Bonasoni et al., 2008). The power required to carry out activities is supplied by 96 photovoltaic panels with 120 electric storage cells, in order to minimize the possible influence of local emissions and guarantee air mass sampling in clean conditions. In cases when the energy obtained from the panels is insufficient (which occurred for 6% of hours during the summer monsoon), additional power is supplied by the photovoltaic panels at the main Pyramid facility where, only in the event of further problems, a diesel-electric generator is available. The only major event of insufficient power occurred on 14–25 June 2007, when two instruments were switched off to save energy for the other instruments. A dedicated satellite connection permits near-real-time data transfer, as well as the remote control of instrumentation. Further details on the measurement site can be found in Bonasoni et al. (2007) and Bonasoni et al. (2008).

2.2 Measurements and sampling procedures

Starting in March 2006, a wide range of measurements for aerosols and trace gas characterisation have been continuously running at NCO-P. In particular, the following instruments are housed in a wood and aluminium shelter:

1. Photometric O_3 analyser (Thermo Electron Corporation – Tei 49C) operating at the wavelength of 254 nm. Data are first stored on a 1-min basis and finally validated as 30-min average values. The sampling methodology was based on the GAW-WMO requirements (GAW, 1992). In particular, during a maintenance campaign on February 2007, the instrument was compared against one of the transfer

standards working at GAW/WCC-EMPA (World Calibration Centre for Surface Ozone, Carbon Monoxide and Methane at the Swiss Federal Laboratories for Materials Testing and Research). This allowed the determination of the combined standard uncertainty, which, following Klausen et al. (2003), was estimated to be less than 2 ppbv in the range 0–100 ppbv.

2. Multi-Angle Absorption Photometer (MAAP 5012, Thermo Electron Corporation) operating at the wavelength of 670 nm, measuring aerosol light absorption. The MAAP calculates absorbance from particles deposited on the filter using measurements of both transmittance and reflectance at two different angles. The absorbance is then converted to the mass concentration of black carbon (BC), using a fixed mass absorption coefficient of $6.6\,\mathrm{m^2\,g^{-1}}$, as recommended by Petzold et al. (2002). The uncertainty in the determined absorbance has been estimated to be 12% (Petzold et al., 2002), while the detection limit was calculated during a field campaign as $3\,\sigma$ of a 12 h blank ($11.16\,\mathrm{ng\,m^{-3}}$).

3. Differential/Scanning Mobility Particle Sizer (DMPS/SMPS) determining the aerosol size distribution for particle diameters from 10 to 500 nm and the Total Particle Count (TPC), with a three-minute time resolution. The SMPS is composed of a ^{63}Ni neutralizer, a custom-made Differential Mobility Analyzer (DMA) (Villani et al., 2008) selecting negatively charged particles, and a TSI Inc. 3010 Condensation Particle Counter (CPC). Sheath and excess flow rates were fixed at $5\,\mathrm{l\,min^{-1}}$, while the aerosol flow rate was determined by the CPC critical orifice at $1\,\mathrm{l\,min^{-1}}$. The aerosol flow rate was monitored continuously to ensure a first step data quality check. The SMPS inversion took into account the CPC efficiency and the charge equilibrium state (Wiedensohler, 1988), using 108 channels over the 10–500 nm range on the up-ramp of the voltage scan. Data quality of the size-distribution was further ensured by comparing the integrated SMPS number concentrations with total concentrations measured by an additional TSI Inc. 3010 CPC, connected to the same sampling line over limited periods. This

Atmospheric Brown Clouds in the Himalayas: first two years of observations

P. Bonasoni et al.

Full Screen / Esc

Printer-friendly Version

Interactive Discussion

comparison indicated that the SMPS was in agreement with the total CPC count within 16±15%, except for nucleation periods, when the two instruments differed because of the high number of ultrafine particles close to the CPC detection limit.

4. Aerosol total and back scattering coefficients at three wavelengths (450, 550 and 700 nm) are derived by an integrating nephelometer (model TSI 3563), installed in March 2006. A $PM_{2.5}$ cyclone limits sampling to aerosol particles with aerodynamic diameter less than 2.5 µm before they enter the nephelometer. Operating procedures follow those described in Anderson and Ogren (1998), in particular for calibration procedures and corrections for truncation errors. The asymmetry factor is then calculated using the method described in Marshall et al. (1995). In addition, due to high relative humidity (RH), especially during the monsoon season (mean RH above 90%), correction procedures recommended by Nessler (2005) were applied. Measurements are performed at $30\,l\,min^{-1}$ with a time integration of 5 min, averaged every hour. Over the course of the 2-year period, a number of problems limited the measurement record: from 1 November 2006 to 10 February 2007, from 10 December 2007 to 25 February 2008. In fact, instrument failures occurred during the autumn and could not be fixed until late winter of the following year.

5. Optical Particle Counter (OPC, GRIMM 190) determining the aerosol size distribution for particle diameters from 0.25 up to 32 µm with an accuracy of 2%, on concentrations over the entire measurement range. The OPC uses a 683 nm laser-diode to illuminate the aerosol beam, and a wide-angle collector optic to detect light pulses with a photodiode. The optical arrangement (mean scattering angle 90°) collects the scattered light with a parabolic mirror (120°). The wide angle optic increases the total amount of scattered light detected by the photo sensor, close to the Rayleigh scattering domain. This improves the signal to noise ratio, which leads to a decrease in the minimum particle size that can be detected (specified by the manufacturer as 0.25 µm). The optic design also smoothes out

Mie scattering undulations caused by the monochromatic illumination, and the sensitivity to particle shape is also reduced. Due to instrument failure, measurements were interrupted on 4 December 2007 and resumed on 5 February 2008.

6. Cimel CE-318 sunphotometer installed at NCO-P at the end of March 2006 within the framework of the Aerosol Robotic Network, AERONET (http://aeronet.gsfc. nasa.gov, EvK^2-CNR site). It provides a characterization of aerosol optical and microphysical properties of the air column above the station. From direct-sun observations the instrument measures aerosol optical depth (AOD) at seven wavelengths (340, 380, 440, 500, 670, 870, and 1020 nm), fine mode ($r <\sim 0.7\,\mu m$) aerosol optical depth at 500 nm (AOD_{FM}), plus total precipitable water (PW) at 940 nm (Holben et al., 1998). Inversion of the measured sky radiance data (almucantars) allows the derivation of other aerosol column properties, such as single scattering albedo (SSA), particle size distribution, asymmetry factor and refractive index (Dubovik and King, 2000). About 11 000 direct-sun observations were collected in the period April 2006–March 2007. Some 7700 passed the cloud-screening process and were employed in the analysis presented by Gobbi et al. (2010).

7. Kipp&Zonen CMP21 pyranometer, measuring downward solar irradiance throughout the 305–2800 nm spectral range. The CMP21 was installed in March 2007. Measurements were interrupted for technical problems in November 2007 and resumed in February 2008. The solar irradiance and instrument body temperatures are acquired every 60 s. The CMP21 has a very good cosine responsivity (cosine error less than 0.4% for solar zenith angles smaller than 80°). The temperature dependence is also small (less than 0.5% within the range $-20\div+50\,°C$), and the spectral responsivity is uniform within the measurement range (95% points at 335–2200 nm). The CMP21 was calibrated at Kipp&Zonen in November 2007, based on the World Radiometric Reference of the World Meteorological Organization. The estimated total uncertainty on hourly irradiance values is less than 2%.

8. High volume aerosol sampler ($30\,\mathrm{m^3\,h^{-1}}$) and low-volume sampler ($1\,\mathrm{m^3\,h^{-1}}$) collecting, non-continuously, particulate matter on quartz fibre filters for off-line chemical analyses. A 10 µm cut-off is applied to the HiVol sampler using a DIG-ITEL PM_{10} pre-separator DPM10/30/00, while a 1 µm cut-off is set for the low-volume sampler using a Digitel DPM10/01/01/0 head. Samplings are routinely carried out, differentiating between night-time and afternoon hours, with the aim of discriminating the aerosol composition impacted by upslope valley breezes from that characteristic of free tropospheric air masses. Off-line chemical analyses included determination of total carbon (TC), organic carbon (OC), elemental carbon (EC) using thermal and thermo-optical methods, water-soluble organic carbon (WSOC) analysis, ion chromatography for inorganic ions and oxalate, and, in the case of PM_{10} samples, atomic absorption spectroscopy (AAS) for determination of Al, Fe, Ca and K.

9. Portable ultra clean air pumps used to fill passivated stainless steel canisters for halocarbons analysis. Samples are collected on a weekly basis, and with higher frequency in the case of intensive campaigns. Off-line analysis of air samples is carried out in gas chromatography-mass spectrometry, preceded by pre-concentration (ADS-GC-MS). Samples are calibrated against working standards (actual air samples), calibrated in turn against the UB98 (University of Bristol) and SIO2005 (Scripps Institution of Oceanography) calibration scales.

10. VAISALA Weather Transmitter WXT510 measuring wind speed and direction, atmospheric pressure, temperature and relative humidity. Precipitation is also measured with a piezoeletrical sensor: this type of sensor can underestimate total precipitation due to the omission of snowfalls.

The sampling of ambient air is performed using four different inlets installed on the shelter roof at about 4 m a.g.l.:

– $PM_{2.5}$ head for nephelometer and DMPS/SMPS instruments (flow rate $1\,\mathrm{m^3\,h^{-1}}$).

- Total Suspended Particle (TSP) head for the optical particle counter ($0.018\,\mathrm{m^3\,h^{-1}}$)

- PM_{10} head for non-continuous high volume aerosol sampling ($30\,\mathrm{m^3\,h^{-1}}$)

- second TSP head for O_3 and BC measurements ($15\,\mathrm{m^3\,h^{-1}}$)

5 - PM_1 head for non-continuous low volume aerosol sampling ($1\,\mathrm{m^3\,h^{-1}}$).

All the atmospheric compound concentrations measured at NCO-P and reported herein refer to STP conditions, while hours of the day refer to Nepal Standard Time, (NST), corresponding to UTC+5.45.

2.3   Air mass back-trajectories and cluster analysis

10 In order to determine the origin of air masses reaching NCO-P, 5-day back-trajectories were calculated every 6 h (at 05:45, 11:45, 17:45 and 23:45 NST) with the Lagrangian Analysis Tool LAGRANTO (Wernli and Davies, 1997). Trajectory calculations were based on the 6-hourly operational analyses produced by the European Centre for Medium Range Weather Forecasts (ECMWF). The 3-D wind fields were interpolated
15 onto a horizontal $1° \times 1°$ grid and are available on 60 hybrid vertical levels. For every point along the trajectory (time resolution: 2 h), the model provides the geographic location and altitude of the air parcel, as well as other important physical quantities, like Ertel's potential vorticity (PV).

Due to the very complex topography of the NCO-P area and the influence of lo-
20 cal/regional transport phenomena related to thermal valley winds, back-trajectory results should be treated with caution. Therefore, in order to capture the dominant synoptic-scale circulation and to minimize the interference of local valley winds, in-situ atmospheric compound behaviours were analysed only as a function of night-time back-trajectories. To better understand the influence of synoptic-scale transport pat-
25 terns on atmospheric compound concentrations observed at NCO-P (see Sect. 4.2),

the LAGRANTO back-trajectories are used in a hierarchical cluster analysis to group the trajectories into clusters. Applying a version of the cluster methodology presented in Dorling et al. (1992), an a-priori number of appropriate clusters was not fixed. At each step of the agglomeration process, the appropriate number of clusters was determined by analysing the variations of specific statistical parameters, i.e. the total trajectory dispersion and the total root mean square deviation (see Tarasova et al., 2007; Dorling et al., 1992). The clustering algorithm was applied to the middle members (MMT) of the LAGRANTO ensemble calculated for the NCO-P pressure level and composed of seven back-trajectories. In particular, following Scheele and Siegmund (2001), the MMT was defined as the ensemble member with the smallest mean square distance to other members, while the intra- and inter-cluster distances were based on the Haversine formula of the great-circle distance between two latitude/longitude points. In this way, a total of 1343 night-time trajectories were analysed during the March 2006–February 2008 period. Since, in the area under consideration, a strong seasonal variation of atmospheric circulation was expected, due to the Asia monsoon, in a first step the cluster analysis was performed on a seasonal basis. Subsequently, to obtain a better description of the seasonal frequency of each identified air mass circulation class, the seasonal clusters were integrated in a yearly categorization by merging similar seasonal clusters.

2.4 Mesoscale modelling using WRF

As shown in the previous section, LAGRANTO back trajectories allow the assessment of the large-scale circulation of air masses arriving at NCO-P. To simulate the meteorology at a scale that captures individual peaks and valleys, nested runs were set up of the Advanced Research (ARW) Version 3 of the Weather Research and Forecast (WRF) model. This is a limited area non-hydrostatic model designed for a range of tasks, from weather forecasting to air pollution transport simulation (Skamarack et al., 2008). The WRF ARW was set up with four levels of nested domains, all centred on Mt. Everest (27.99° N, 86.93° E). The coarsest-resolution (27 km) outermost domain

covers much of South Asia and the Tibetan Plateau, while the innermost domain (3 km resolution) covers the Khumbu and adjoining regions.

The model is driven at the boundary of the outermost domains by NCEP Final Analysis (FNL) analyzed meteorology, available at six hourly intervals at $1° \times 1°$ horizontal resolution on 27 vertical levels. The nested domains have two-way interactions with each other. Model physics are parameterized using a simple ice scheme, and a Goddard scheme for shortwave radiation (Chou and Suarez, 1994). Cumulus clouds are parameterized in the outer two domains using a Kain-Fritsch scheme (Kain, 2004), where they are recalculated every 5 min. They are calculated explicitly in the inner two domains. The bottom boundary has a 4 layer Noah land surface model. Surface land use and topography data is ingested at 30 arc-second resolution, and interpolated to the model grid by the WRF pre-processor. In the region around Mt. Everest, the default USGS 30 arc-second digital topography database normally used by WRF contains excess smoothing, which results in a loss of the actual shape of the topography. For example, the Mt. Everest, Lhotse, and Nuptse reliefs are merged into one large dome shaped mountain, while deep tributary valleys are merged together into one large basin. Thus, an accurate simulation of the Khumbu valley meteorology for the analysis of air-mass transport to NCO-P involved correcting the elevation of the bottom boundary. Use was made of a gap-filled version of the NASA Shuttle Radar Topography Mission (SRTM) 3 arc-second database obtained from http://www.viewfinderpanoramas.org, averaged to 30 arc-seconds, to correct the elevation data employed by WRF from $26°$ to $28°$ north, and $86°$ to $88°$ east. The domain of the third nest level of the present WRF simulation, covering a 300 km by 300 km area centred on Mt. Everest, is shown in Fig. 2, where the NCO-P location is marked by a red dot, located at grid points (46.3, 49.7).

3   Meteorological characterization and air mass circulation

3.1   Seasonal weather regime behaviour

The Himalayan high-altitude climate is intensely characterised by its relationship with large-scale circulation, and strongly dominated by the diurnal cycle of thermal parameters (Bollasina et al., 2002). In fact, at NCO-P, the seasonal variation of atmospheric conditions is influenced both by the local mountain wind system (with a strong diurnal valley wind and a weak mountain night-breeze), and by the large-scale Asian monsoon circulation. In particular, besides determining the seasonal variations of the meteorological parameters, the annual variations of the main synoptic circulation can also modulate the diurnal cycles characterizing the local mountain weather regime (Barros and Lang, 2003; Ueno et al., 2008).

Time series of atmospheric pressure, air temperature, relative humidity, rain precipitation, wind speed and direction are shown in Fig. 3 for the period from March 2006 to February 2008.

3.1.1   Atmospheric pressure (AP)

As shown in Fig. 3a, AP behaviour has an average value of 550.9±3.6 hPa (±1 sigma), characterized by higher (and less variable) values from June to August (average value: 552.4±1.4 hPa) and lower (and more variable) values from November to March (average value: 546.8±3.9 hPa). Such behaviour reflects the development of the "Tibetan High" during summer in the upper troposphere and the oscillations of the Subtropical Jet Stream (SJS), as well as the passage of eastward propagating synoptic disturbances during the rest of the year (Bohmer, 2006; Schiemann et al., 2009). The daily behaviour of AP shows a systematic semidiurnal variation characterised by an amplitude of about 1–2 hPa, with diurnal maxima at 10:00–22:00 NST and diurnal minima at 04:00–16:00 NST. This semidiurnal pressure cycle, with highest amplitude during January–February (∼2.2 hPa) and lowest during June–August (∼1.0 hPa), had already

been observed in Himalayas (Ueno et al., 2002) and at other high altitude sites (e.g. Petenko and Argentini, 2002). It was explained in terms of the atmospheric tidal theory, relating to the warming of upper atmospheric layers due to the interaction between O_3 molecules and solar radiation (Chapman and Lindzen, 1970).

3.1.2   Air temperature (T)

During the considered period, T showed a mean value of $-3.0 \pm 4.5\,^{\circ}$C and exhibited a seasonal behaviour (Fig. 3b) characterised by a maximum during the summer period (average value: $1.7 \pm 2.1\,^{\circ}$C), the highest values being in July (even above $8\,^{\circ}$C). Lower T values were recorded during winter (average value: $-6.3 \pm 4.5\,^{\circ}$C), the lowest being observed in January–February (below $-15\,^{\circ}$C). Such behaviour agrees well with the analysis of the SJS location and 500 hPa geopotential height carried out in the light of the ECMWF analysis. In fact, since the SJS determines the northern limit of warmer subtropical air, it is realistic to expect an increase of air temperature when the SJS moves northward of the Himalayas (from May to September). By contrast, from October to February, the SJS is located at lower latitudes and the Himalayan range can be affected by cold air mass irruptions. For instance, this was the case in January 2007, when the lowest T daily value ($-18\,^{\circ}$C) was recorded at NCO-P. However, as suggested by the high standard deviation, during the cold months, T showed a large variability with daily values even above $-1\,^{\circ}$C. Such "warm events" were already highlighted by Ueno and Pokhrel (2001) and Bollasina et al. (2002), and have been related to the passage of synoptic disturbances affecting the high Khumbu valley region, transporting warmer, moister air masses from the Arabian Sea (Ueno et al., 2002). This could be the case also of NCO-P, because "warm events" are also characterised by significant simultaneous variations of AP and RH average daily values (Fig. 3a, c).

Atmospheric Brown Clouds in the Himalayas: first two years of observations

P. Bonasoni et al.

3.1.3 Relative humidity (RH)

The RH behaviour at NCO-P (Fig. 3c) was characterized by a clear seasonal cycle, with very low values in the period from the end of November to January/February (average value: 22±14%) and high values from the end of May to the end of September (average
5 value: 94±4%). Since RH behaviour in the Southern Himalayas is strongly influenced by the South Asian monsoon cycle due to the transport of moist air masses from the Indian Ocean (e.g., Krishnamurti and Bhalme, 1976; Barros and Lang, 2003), this parameter was used to evaluate the monsoon phase over the considered region.

3.1.4 Rain precipitation (PRP)

10 The analysis of the PRP time-series (Fig. 3d) also highlighted the seasonal influence of the summer monsoon at NCO-P. At the measurement site, monsoon precipitations (237 mm in 2006 and 238 mm in 2007) were characterised by light showers or drizzles, more frequent in the evening and at night, while only sporadic events with heavier rain (>10 mm/day) were detected (Fig. 3d). However, it should be noted that such values
15 could be underestimated due to the loss of snowfall (see Sect. 2). This would also explain the absence of any signal of precipitation from November to April, when 92% of 30-min observations showed air-temperatures below 0°C.

3.1.5 Wind speed (WS)

During the investigated period, daily values of WS were characterised by an average
20 value of $4.7\pm1.0\,\mathrm{m\,s}^{-1}$ (Fig. 3e). Thus, despite its elevation, the measurement site does not appear to be an extremely windy location, thanks to the sheltering effect of the mountain ridge. Wind speed above $6\,\mathrm{m\,s}^{-1}$ was mainly observed from November to May, and was probably due to the passage of synoptic disturbances (see, for instance, the simultaneous AP decrease on 22 November 2006 or on 24 January 2008). On
25 average, these months appeared slightly more "gusty" (standard deviation: $1.1\,\mathrm{m\,s}^{-1}$)

compared to summer months (standard deviation: $0.6\,\mathrm{m\,s^{-1}}$), probably as a result of the more effective occurrence of the subtropical jet stream (SJS) over the Southern Himalayas.

3.1.6 Wind direction (WD)

At NCO-P, WD showed a bidirectional distribution, with dominating directions from the bottom of the valley (S-SW) and from the upper mountain (N-NE). This was related to the development of a strong mountain-valley breeze regime (Bollasina et al., 2002), brought about by the thermal heating of valley and mountain slopes (e.g. Henne at al., 2005). For most of the year (October to May), valley winds prevailed during day-time, while mountain winds prevailed during night-time (Fig. 3d). During the summer months, due to the large scale forcing of the South Asian monsoon (Ueno et al., 2008), valley breeze winds are predominant also during night-time. This was reflected by the seasonal frequency of valley winds, which was characterised by an 80% occurrence from June to September and a 45% one from November to April. Due to this abrupt change in local circulation, WD was also used to define the monsoon phase over the considered region.

3.2 Identification of season transitions

In the present work, sudden variations in the mountain weather regime (as defined by RH and WD behaviour) were used to identify the onsets and the decay dates of the summer monsoon and winter seasons.

The winter season was identified when daily RH values never exceeded 70%, and northerly mountain winds were well established during night-time. In agreement with Ueno et al. (2008), the monsoon season was defined as the period characterised by high humidity levels, and the presence at the measurement site of southerly wind, also during night-time. In fact, from May to September, an evident decrease in the frequency of mountain winds was observed, and southerly winds could prevail even

Title Page

Abstract | Introduction

Conclusions | References

Tables | Figures

◄ | ►

◄ | ►

Back | Close

Full Screen / Esc

Printer-friendly Version

Interactive Discussion

during night-time. As suggested by Barros and Lang (2003) and Ueno et al. (2008), this change in local circulation could represent the in-situ evidence for the onset of the large scale summer monsoon flow from the Indian plains to the Tibetan Plateau. In good agreement with the analyses of Rajeevan and Revadekar (2007, 2008), the combined analysis of RH and wind regime changes led to the seasonal definition reported in Table 1. It should be noted that the onset dates of the monsoon season, as defined in this way (21 May 2006 and 6 June 2007), are ahead of the onset of the rainy season at NCO-P by about two weeks. In fact, Bollasina et al. (2002) identified 12 June as the average onset date for summer monsoon precipitation, analysing six-year (1994–1999) of daily precipitation data at this site. Our results are in good agreement with those of Ueno et al. (2008) and Barros and Lang (2003), showing that in the Southern Himalayas significant changes in mountain weather regime relating to the summer onset of the large scale southern monsoon circulation strongly anticipate the precipitation onset.

3.3 Sky conditions and cloud classification

To identify cloud-free and cloudy periods at NCO-P from pyranometer measurements, a simple algorithm was implemented. First, a cloud-free day characterized by low aerosol and pristine conditions were identified. Following Long and Ackermann (2000), the measured irradiance was fitted with the expression

$$I(\theta) = A[\cos(\theta)]^{\alpha}$$

where θ is the solar zenith angle, and A and α are constants. The standard deviation σ of the ratio R between the observations and the fitting curve at the corresponding solar zenith angles was calculated over 10-min intervals. The observations whose value of σ exceeded a fixed threshold (0.005) were labelled as cloudy. In addition, because the irradiance variability was small in a few cases of overcast sky with thick cloud, cases with measured irradiances outside a 20% range of the clear-sky fitting curve were also labelled as cloudy. Only cases with solar zenith angle smaller than 70° were

considered, since shadowing of the sensor by mountains sometimes occurred during the year for larger values of θ. The method is efficient in identifying clouds, and results agree well with determinations of cloudy periods based on visual inspection of the daily course of measured irradiances by an experienced operator. Cloudy periods were fur-

5 ther separated into classes, qualitatively identified as thin/moderate, thick, or scattered, depending on the value of R. Thick clouds are those corresponding to $R \leq 0.5$. According to the algorithm of Barnard and Long (2004), $R = 0.5$ roughly corresponds to a cloud optical depth of 8 over a surface not covered by snow or ice. Figure 4 shows the frequency of occurrence of the different conditions during the day, summed over

10 the main seasons identified above. Due to the limit on the value of θ, information after 15:00 NST for the post-monsoon season is not available. The sky conditions clearly show different behaviours during the four seasons, in response to large scale dynamical phenomena. The average daily evolution in the different seasons sometimes shows a strong diurnal cycle, partly determined by local circulation. Thick clouds were present

15 in up to 50% of the cases in the afternoon during the pre-monsoon and, consistently with the precipitation data reported in Fig. 3d, their occurrence increased during the monsoon season, with a frequency of about 80% in the mid-afternoon. Thick clouds were found to be less frequent in the post-monsoon, and rare during the winter season. As expected, cloud-free skies are most common in the winter season, while their fre-

20 quency is smaller than 10% during the monsoon period. A distinctive daily behaviour appears, with cloud-free conditions occurring mostly during the morning throughout the year. Thin/moderate clouds seem to display a smaller daily evolution, particularly in the pre-monsoon season. The diurnal cycle is large in the non-monsoon seasons, while it is reduced during the monsoon, as an effect of the interaction between large scale and

25 local circulation, and the influence of cloudy conditions (present in more than 90% of cases throughout the day) on valley wind development .

3.4 Local circulation description

At NCO-P the wind regime was characterised by an evident mountain/valley breeze circulation, as shown by the analysis of the southern wind component (Vy) from post-monsoon to pre-monsoon (Fig. 5, upper plate), while in the monsoon season southerly winds were predominant. During the pre-monsoon season, valley winds ($Vy > 0$) were evident from about 09:00 to 20:00 NST, and from 09:00 to 18:00 NST during the post-monsoon and winter season. The slightly stronger valley winds observed in the afternoon during the pre-monsoon can be explained by the stronger driving force caused by the more efficient ground heating (Bollasina et al., 2002). During night-time, the wind flow reversed ($Vy < 0$) but showed lower intensity compared to the day-time valley winds. This mountain wind system clearly influenced the diurnal behaviour of moisture at the measurement site. In fact, even if the diurnal variation of Specific Humidity (SH, Fig. 5, middle plate) was small when compared to seasonal variation (from about $1\,\mathrm{g\,kg^{-1}}$ during the Winter season to 3–$4\,\mathrm{g\,kg^{-1}}$ during the pre-monsoon and post-monsoon), the valley breeze favoured the transport of moisture from lower altitudes during day-time, the highest SH values (about 3–$4\,\mathrm{g\,kg^{-1}}$) being recorded from 16:00 to 18:00 NST . The pre-monsoon evolution of local wind fields around NCO-P was confirmed by WRF simulations for a selected day (30 March 2006). In particular, while at 03:00 NST the measurement site experienced northerly flows coming from the Tibetan Plateau, at 15:00 NST, following ground heating, up-valley winds coming up from the Dudh Koshi and Khumbu valleys dominated at the NCO-P location (Fig. 6, upper panels).

During the monsoon season, significant changes of the local wind regime were observed at NCO-P, bringing moisture from the bottom to the top of the Khumbu valley, due to the strong heating of the ground and the consequent release of large quantities of latent heat into the atmosphere. The average diurnal variation of Vy showed increasing values in the morning (with the valley breeze) and a maximum around midday, with decreasing values until night, when the southerly winds were still observed at

Title Page

Abstract | Introduction

Conclusions | References

Tables | Figures

◄ | ►I

◄ | ►

Back | Close

Full Screen / Esc

Printer-friendly Version

Interactive Discussion

the measurement site (Fig. 6). As shown by WRF simulations for a specific monsoon day (15 July 2007), during day-time the up-valley wind observed at NCO-P was related to very pronounced flows onto the Tibetan Plateau, which originated from the lower valleys of Nepal (Fig. 6, bottom panels). Also during night-time (03:00 NST), the upper reaches of the valleys continue to show a southerly flow towards the Tibetan Plateau (Fig. 6, bottom panels). This is in agreement with previous investigations by Ueno et al. (2008) and Barros and Lang (2003), suggesting that during night-time the measurements carried out at NCO-P can be representative of the large-scale monsoon flow between the Indian plains and Tibetan Plateau. During the monsoon season, the day-time valley breeze showed a gentler decreasing trend toward the evening (Vy, Fig. 6), probably due to the "pumping effect" of the latent heat release relating to water vapour condensation on cumulous clouds (Bollasina et al., 2002). During this season, the SH diurnal variation characterized by high values (in average above $7\,g\,kg^{-1}$) with maximum after midday, indicated the efficient transport of moist air masses from the bottom of the valley, with a larger presence of clouds at NCO-P. This was further confirmed by the analysis of solar irradiance (Fig. 5), which showed lower irradiance levels during the monsoon (average value at 12:00 NST: $832\pm342\,W\,m^{-2}$) than in other seasons (average value at 12:00 NST: $954\pm242\,W\,m^{-2}$).

3.5 Large scale circulation description

Located on the south-facing side of the Himalayas, the upper Khumbu valley is particularly affected by large scale circulation. In fact, signals of the so-called Tropospheric Biennial Oscillation (Webster et al., 1998) were found by Bertolani et al. (2000) analysing in-situ meteorological parameters at the Pyramid International Laboratory, while Bollasina et al. (2002) showed a clear link between intra-seasonal precipitation variation in the upper Khumbu valley and large-scale circulation modes. In this area, the seasonal weather behaviour depends on variations in the "Tibetan High", a strong thermal anticyclone forming in the upper troposphere during summer season, and correlating with the strength and location of the SJS during the rest of the year (Krishnamurti and Bhalme,

1976; Bertolani et al., 2000; Ueno et al., 2001). During the cold season, from October to May, the low-level cold Siberian high controls the weather over much of Asia, while in the upper troposphere the axis of the SJS is just south of the Himalayas, and synoptic disturbances travel eastward affecting the southern slope of this mountain ridge (Ueno et al., 2001). Moving into summer, the SJS starts to oscillate between northern Tibet and the southern Himalayas (Barros and Lang, 2003). This leads to a weakening of general flows, which can provide favourable conditions for the development of daytime convection over the southern Himalayas, thus modulating the onset of the summer monsoon rainy season (Barros and Lang, 2003; Ueno et al., 2008). In June–August, the SJS is situated in northern Tibet, and the "Tibetan High" becomes the predominant synoptic pattern at upper levels. The migration of monsoon depressions from the northern Gulf of Bengal (Ueno et al., 2008) and the low-level cross-equatorial jet (Krishnamuti and Bhalme, 1976) may influence the regional weather and total column moisture over the Himalayas. In fact, as deduced by sun-photometer measurements (Fig. 7), a strong annual cycle characterized the precipitable water (PW) at the EvK^2-CNR Aeronet site at NCO-P. While low PW values were observed from October to May, higher values characterized the atmospheric moisture from June to September. This is consistent with the transport along the northern flank of the low-level westerly jet of air-masses rich in moisture from South/South-East to eastern Nepal and southern Himalayas during the summer period (Barros and Lang, 2003).

The air-mass flows specifically characterising the NCO-P region for each season are depicted in Fig. 8, showing the field concentrations of the LAGRANTO back-trajectory points calculated along the period 1 March 2006–18 February 2008. To emphasize the transport paths also on "peripheral" regions far away from the measurement site, a logarithmic scale is adopted. From the analysis, it is evident that: (a) during the winter season NCO-P is mainly affected by a very fast westerly circulation related to the well-developed SJS along 30° N; (b) during the pre-monsoon and post-monsoon, slower but still westerly air-masses mainly affected the measurement site with evident excursions related to SJS undulation and synoptic scale systems; (c) during the monsoon season

P. Bonasoni et al.

NCO-P is strongly affected by air masses originating at lower latitude regions (i.e. Gulf of Bengal and Indian sub-continent). The analysis magnifies the different atmospheric circulation characterising the high Himalayas with respect to the South Asia plains during the winter and transitional seasons. While in the South Asia boundary layer, a north to north-easterly circulation usually prevails, in the middle and upper troposphere the mean flow turns to westerly (Phandis et al., 2002), thus indicating a synoptic-scale decoupling of the middle troposphere circulation from the lower troposphere. To investigate the synoptic-scale circulation at the measurement site, and to identify possible relationships between different air mass paths and atmospheric compound variations at NCO-P (see Sect. 4), a cluster analysis was applied to night-time LAGRANTO back-trajectories (see Sect. 2.3).

Depending on the geographical origin and paths of the analysed back-trajectories, 7 clusters were identified, divided into three main classes: SW south-westerly (SW-AP: Arabian Peninsula, SW-AS: Arabian Sea, SW-BG: Bengal Gulf); W westerly (W-NA: North Africa, W-EU: Europe, W-ME: Middle East); and REG regional, as shown in Fig. 9. Significant variations in the cluster frequencies among the different seasons were found, as shown by the seasonal cluster analyses at NCO-P for the period March 2006–February 2008 (Fig. 10) and in agreement with previous investigations (e.g. Böhmer et al., 2006). In particular, the three "W" clusters characterised 43.3% of the investigated period (Fig. 9), suggesting the prevalent role of the SJS and westerly synoptic scale systems in influencing the atmospheric circulation over the southeastern Himalayas (particularly during non-monsoon seasons). The obtained cluster analysis also showed a not negligible contribution on the part of the "SW" circulations, which were established at NCO-P for 23.5% of the analysed period. According to Böhmer et al. (2006) and Barros and Lang (2003), these circulation classes are related to the passage of synoptic-scale disturbances over the western Indian subcontinent and Himalayas (SW-AS and SW-AP) during non-monsoon seasons, and to the development of the well-established monsoon circulation over the Gulf of Bengal (SW-BG) during the monsoon season, promoting synoptic-scale air mass uplift, as also shown

by the cluster vertical cross-sections (Fig. 9). Similar cross-section depicted by REG circulation (33.2% of clusters, Fig. 9) stressing the possible uplift of regional polluted air-mass observed at the measurement site during the 2-year period (Fig. 10). In order to assess the possible influence of regional emissions on the atmospheric compounds observed at the measurement site, it is worth noting that not-negligible REG contributions were also present in the pre-monsoon and post-monsoon seasons even if the most important contribution was related to the summer monsoon (Fig. 10). However, this type of circulation was not present during the winter season, when the main synoptic transport flow to NCO-P usually occurred in the free-troposphere (Fig. 9), further attesting the predominant influence of the SJS during this period.

Also noteworthy is the strong circulation change associated with the South Asian summer monsoon, causing the NCO-P station to be almost solely affected by "SW" (SW-BG) and "REG" air masses (96.1% of frequency in total). This suggests the important role played by depressions migrating from the Gulf of Bengal (Ueno et al., 2008) and the low-level monsoon trough (Krishnamuti and Bhalme, 1976; Bollasina et al., 2002) in determining air mass transport towards the measurement site during this season.

4   Atmospheric composition at NCO-P and possible influence of the Atmospheric Brown Cloud

The long dry season in the South Asian region, and the persistent subsidence and trade wind inversion characterising the winter and pre-monsoon seasons, strongly inhibit the ventilation and dilution of pollutants, favouring their build-up in the lower troposphere (Ramanathan et al., 2008). Such meteorological conditions also promoted ideal conditions for the onset of wildfires, which represent an additional important source of BC and O_3 precursors in atmosphere (Novelli et al., 2003; Bond et al., 2004). Aerosol and gaseous pollutants in layers of brownish haze cover the vast Indian sub-continent during the winter and pre-monsoon period, forming the so-called Atmospheric Brown

Atmospheric Brown Clouds in the Himalayas: first two years of observations

P. Bonasoni et al.

Title Page

Abstract	Introduction
Conclusions	References
Tables	Figures

◀◀   ▶▶

◀   ▶

Back   Close

Full Screen / Esc

Printer-friendly Version

Interactive Discussion

Cloud (Ramanathan et al., 2007). On the Indian sub-continent, alongside anthropogenic pollution, dust aerosols also build up in the pre-monsoon and monsoon seasons (Liu et al., 2008).

Because the NCO-P atmospheric observations constitute the first continuous atmospheric characterization in the high Himalayas, as well as providing an overview of the seasonal variations of anthropogenic and natural atmospheric compounds (BC, O_3 and coarse particle numbers, Dp>1 µm), the following discussion also focuses on the possibility that local/regional and synoptic atmospheric circulations might favour the transport of Brown Cloud pollutants to the Himalayas and their glaciers. For the three considered compounds, the observed seasonal variation values (Table 2) and behaviours shown in Fig. 11, magnify the role of the South Asia summer monsoon cycle in determining the characteristics of atmospheric composition at NCO-P, even if short time variations (on synoptic scales) are also evident (Fig. 11). These marked "acute events" also influenced the BC yearly averaged concentrations at NCO-P (160 ng m^{-3}), which are similar to values obtained by measurements carried out at NAM CO, a station located on the Tibetan Plateau (4730 m a.s.l.) (J. Ming, personal communication; Marinoni et al., 2010). The monsoon season was characterized by the lowest seasonal BC concentrations (50 ng m^{-3}), a value comparable with the European continental background, as reported by Marinoni et al. (2010), while a clear maximum during the pre-monsoon period was observed.

Surface ozone concentrations (yearly mean: 49 ppbv) also exhibit a clear seasonal cycle at NCO-P (Fig. 11), with high values during the pre-monsoon and lower values during the monsoon period (Table 2). In general, the average O_3 diurnal cycles presented different shapes in the different seasons, suggesting a considerable interaction between the synoptic-scale circulation and the local mountain wind regime (Cristofanelli et al., 2010). A similar seasonal behaviour is found when observing the median values of coarse particle concentrations, even if the analysis of seasonal mean values suggests that the monsoon period may be more influenced by dust transport events than the post-monsoon.

4.1 Atmospheric composition during the monsoon period

During the monsoon, 96% of air-masses reaching NCO-P were related to synoptic-scale uplift (Figs. 9 and 10) within the REG (74%) and SW-BG (22%) clusters. The specificity of summer monsoon air-mass circulation at the measurement site was strengthened by the SW-BG air-mass circulation, which, usually associated with strongly precipitating low pressure systems over the Bay of Bengal (Barros and Lang, 2003), influences NCO-P only during this season. Conversely, when westerly shifts in the monsoon circulation occurred, large amounts of anthropogenic pollutants (i.e. BC and O_3) and mineral dust can be transported from the Western Indo-Gangetic plains towards the Himalayas and NCO-P, as recorded on 12–22 June 2006 (Bonasoni et al., 2008).

As deduced from LAGRANTO back-trajectories (Figs. 9 and 10), this synoptic circulation favoured the transport of clean air-masses, also coming directly from the Bay of Bengal. Accordingly, very low BC, coarse aerosol and O_3 concentrations (about 1/6, 1/4 and 1/2 with respect to pre-monsoon mean values, respectively) characterized the measurement site, as reported in Table 2. Enhanced wet scavenging and decrease of emissions from domestic heating, which commonly affect the region during summer, can significantly contribute to reducing the aerosol concentration in air-masses transported to NCO-P, as also shown by Marinoni et al. (2010), Sellegri et al. (2010) and Decesari et al. (2010). The significant role played by the South Asia monsoon in determining O_3 summer concentrations, the wash-out of the O_3 precursor and the meteorological conditions not favourable to an efficient photochemical O_3 production (Agrawal et al., 2008), are also reflected in the low O_3 concentrations measured at NCO-P during the monsoon (Table 2). Similar O_3 behaviours have been observed at other mountain stations in this continental area, e.g. Mt. Abu, in India (Naja et al., 2003) and Mt. Tai and Mt. Huang, in eastern China (He et al., 2008).

4.2 Atmospheric composition during non-monsoon seasons and influence of Atmospheric Brown Cloud

A pronounced change in atmospheric composition properties occurred at NCO-P in the passage from the monsoon to post-monsoon period, as shown by O_3 and BC seasonal values in Table 2. Significant increases in O_3 and BC were observed at the measurement site in the post-monsoon season. They became increasingly marked in winter and the pre-monsoon season (Fig. 11), following the change in weather conditions and atmospheric circulation (Figs. 8 and 9). In fact, most of the post-monsoon (56%) and winter (77%) was characterised by westerly air-masses, as indicated by LAGRANTO analyses (Fig. 9). Similar behaviour was also found for PM_1 and coarse mass values (Marinoni et al., 2010), and was evident in the amounts of chemical compounds investigated by Decesari et al. (2010), which indicated a large contribution from carbonaceous aerosols, and, to a lesser extent, from nitrate and sulphate. During the cold-dry winter and pre-monsoon seasons, domestic heating and cooking, open biomass burning and energy production favour anthropogenic emissions of large amounts of aerosols and pollutants in the atmosphere, encouraging the formation of the Brown Cloud on the Indian plains (Ramanathan et al., 2008). As indicated by Gautam et al. (2009), strong westerly winds can lead these pollutants to accumulate with mineral dust over the Indo-Gangetic plain towards the Himalayan foothills (Fig. 1), subsequently transporting these air masses up to NCO-P. This transport is more effective in the warmer season (pre-monsoon), when the atmospheric boundary layer attains greater thickness.

During non-monsoon seasons, the maximum seasonal O_3 concentration (60.9±8.4 ppbv) was registered during the pre-monsoon period (Table 2). Due to the station's high altitude, a not negligible contribution to surface O_3 concentration (19.2%) was related to stratospheric air-mass intrusions (SI), which affected the measurement site for about 20% of pre-monsoon days (Cristofanelli et al., 2010). Nevertheless, for O_3, as for BC, an influence of anthropogenic emissions was likely, as suggested by Ramanathan et al. (2007), who observed, over India and South Asia, the strongest

influence of the Brown Cloud from November to April. As reported in Table 2, high coarse particle concentrations also affected NCO-P during the pre-monsoon period. Air-masses rich in mineral aerosol supplied by dust storms in desert areas, or from vast dry fallow agricultural lands, can plausibly affect the slopes of the southern Himalayas during the pre-monsoon period, as suggested by previous investigations (Prasad and Singh, 2007; Liu et al., 2008a; Gautam et al., 2009). This is confirmed by Duchi et al. (2010) and Decesari et al. (2010), who indicate that air masses rich in mineral dust coming from Pakistan/Afghanistan and the Indo-Gangetic plains may play an important role in determining both coarse aerosol concentrations and PM_{10} values at NCO-P.

4.2.1 Influence of local/regional circulation on atmospheric composition at NCO-P during the pre-monsoon period

The transport of high levels of pollutants to the high Himalayas is efficiently accomplished by transport processes on both the local/regional-and long-range scales. Particularly in the pre-monsoon season, the Khumbu valley represents an efficient and persistent channel for the transport of large amounts of absorbing particles to NCO-P, carried by the day-time up-valley breeze, as suggested by the analysis of average BC and PM_1 diurnal variations presented by Marinoni et al. (2010). Shortly after sunrise, pollutants start to rise, reaching a maximum in the late afternoon ($\sim$600 ng m^{-3} for BC and 6 µg m^{-3} for PM_1, with average diurnal amplitude between 2 and 5) (Marinoni et al., 2010). Such diurnal behaviour was well correlated with the behaviour of specific humidity (SH) (Sect. 3.4 and Fig. 6), indicating that polluted air-masses coming from the lower troposphere can reach the measurement site under valley wind breezes. This possibility is well traced by WRF model simulations (Sect. 3.4), and is further supported by Decesari et al. (2010), who show the existence of a clear difference in the chemical composition between night-time and afternoon samples of both PM_1 and PM_{10} filters.

In view of the above considerations and of experience gained in other mountain areas (e.g. Carnuth et al., 2002; Henne at al., 2004), the present observations suggest that Himalayan valleys could represent a "natural chimney" through which Brown Cloud

pollutants can be directly vented to the high Himalayas and middle/upper troposphere. The "natural chimney" effect is probably induced by thermal circulation. Thus, with the purpose of accurately determining its contribution to the high BC values observed during the pre-monsoon season, days on which the diurnal breeze cycle was well developed were identified, by singling out the days that showed significantly higher afternoon than night-time SH values, as also applied by Zellwegger et al. (2003) and Henne at al. (2008). From this pre-monsoon analysis 183 days were found to be influenced by local breeze circulation, confirming that about 90% of the days were characterized by the "natural chimney" effect. On such days, significantly higher daytime BC values ($625.0\,\mathrm{ng\,m^{-3}}$) and diurnal amplitude ($441.9\,\mathrm{ng\,m^{-3}}$) were observed as compared to the remaining days ($317.0\,\mathrm{ng\,m^{-3}}$ and $141.6\,\mathrm{ng\,m^{-3}}$, respectively), indicating that when up-valley winds were well-developed, the BC concentration observed at NCO-P was at least double. However, it should be noted that the BC concentrations seem to decrease strongly with altitude. In fact, the BC values registered at the central Himalayan Nainital station (1950 m a.s.l.) during the winter of 2004 ($1.36\pm0.99\,\mathrm{\mu g\,m^{-3}}$), were significantly higher than NCO-P ones, while BC concentrations in India ranged from few $\mathrm{\mu g\,m^{-3}}$ to $27\,\mathrm{\mu g\,m^{-3}}$ (Marinoni et al., 2010).

Despite BC, surface O_3 did not show any significant average diurnal variation during the pre-monsoon period (Cristofanelli et al., 2010). This suggests that, on a seasonal basis, the contribution of polluted air-masses carried from the lower troposphere by up-valley breezes was similar to that coming from the upper troposphere via nighttime down-valley breezes, without ruling out the possibility that the Himalayan free troposphere could be characterized by O_3 amounts directly connected to polluted air mass venting and recirculation processes.

4.2.2 Influence of synoptic circulation on atmospheric composition at NCO-P during the pre-monsoon period

For the purpose of evaluating the possible influence of synoptic-scale air-mass concentrations on the atmospheric composition observed at NCO-P during the pre-monsoon

phase, BC and O_3 data were analysed as a function of the mass cluster classification presented in Sect. 3.5. To avoid interaction with local valley wind, only night-time (i.e. between 22:00 to 06:00 NST) data was considered. In addition, in order further to exclude data possibly influenced by local emissions from combustion processes, observations characterised by the presence of BC "spikes" in 3-h night-time values (i.e. BC>431 ng m^{-3}, corresponding to 95th percentile) were also neglected. The results obtained are shown in Table 3.

The seasonal pre-monsoon highest O_3, BC and coarse particle median values (68 ppbv, 124 ng m^{-3} and 0.44 cm^{-3}, respectively) were recorded for the W-ME air-masses, whose values were well above the median values observed at NCO-P during the pre-monsoon night-time (61 ppbv, 100 ng m^{-3}, and 0.14 cm^{-3}). This suggests that, alongside the influence of up-valley winds, the synoptic circulation also significantly affects concentrations of anthropogenic pollutants and mineral dust in the pre-monsoon season. Moreover, the W-ME selection was also characterised by the greater occurrence of concentrations above the seasonal 75th percentile (conditional probabilities: 42%, 34% and 58%, respectively). Even if the W-ME cluster presents a 19% frequency during the pre-monsoon period (Fig. 9), it is clear that air-masses containing the highest concentrations of pollutants are associated with this circulation.

This is in agreement with the results of Mühle et al. (2002), who pointed out that a significant amount of pollution can characterise the mid-latitude free troposphere over the Arabian Peninsula and Middle East. The Middle East region is a significant source of anthropogenic emissions and photochemical air pollution (Lelieveld et al., 2009; de Laat et al., 2001), as well as a considerable dust source area (Washington et al., 2003; Prospero et al., 2002). The presence of large amounts of anthropogenic pollutants and mineral dust over the Indo-Genetic plain during the pre-monsoon period was observed by Ramanathan et al. (2008) and Prasad et al. (2007). As shown by the cluster analysis (Fig. 10), under W-ME circulation it is likely that such pollutants reach NCO-P after being vented into the free troposphere. Liu et al. (2008) observed dust layer depths up to 3–6 km over the Indian sub-continent for about 44% of cloud-free periods, indicating

that natural and anthropogenic emissions from the surface may be injected into the free tropospheric circulation. High pollution layers had already been observed by Verma et al. (2006) over the Indian sub-continent, as high as 600 hPa in the presence of strong upward motions along southern Asian coastlines during winter-spring. As proposed by Raman et al. (2002), continental outflow of pollutants driven by the surface level northeast monsoon winds can be lifted into the free troposphere by the strong land-sea breeze circulation which characterises the western Indian coastlines. As analysed by Phandis et al. (2002) in the NCEP reanalysis at 1000 hPa for February 1999, strong north-easterly winds also flow over the northern coastlines of the Arabian Sea. Thus, it was hypothesized in the present work that land-sea diurnal breezes and the continental outflow from the western Indo-Gangetic plain and Arabia could affect air-masses flowing towards NCO-P under W-ME circulation (Fig. 9). Consequently, it was also likely that aerosol and O_3 transported from polluted Arabian, Persian Gulf region and Indian subcontinent significantly affected the behaviour of atmospheric compounds observed at NCO-P under W-ME circulation. The possible influence of these regions as emitters of pollution in the southern Himalayas was also supported by the high BC concentrations (124 and 101 $ng\,m^{-3}$) observed when W-ME and SW-AP air-masses affected the measurement site. Given that W-ME air masses could cross other large arid areas (i.e. Iran, Turkmenistan and Afghanistan/Pakistan) before reaching the measurement site, relatively high calcium and low iron, considered fingerprints for mineral dust originating from India-Pakistan deserts, were found in the PM_{10} at NCO-P (Decesari et al., 2010), confirming the path of such air masses (Decesari et al., 2010 and references therein). During pre-monsoon W-ME circulation, the surface O_3 analysis performed by Cristofanelli et al. (2010) shows that 26% of observations were probably influenced by air-mass transport from the stratosphere, suggesting that this contribution cannot be excluded for the high O_3 concentrations observed at NCO-P. During the biomass burning spring-time season, plumes rich in BC and O_3 can be rapidly transported into the free and upper troposphere from western Asia and north Africa, as already pointed out by Sudo and Akimoto (2007) and Verma et al. (2008). Due to the dominant westerly

ACPD

10, 4823–4885, 2010

Atmospheric Brown Clouds in the Himalayas: first two years of observations

P. Bonasoni et al.

Title Page

Abstract | Introduction

Conclusions | References

Tables | Figures

|◄ | ►|

◄ | ►

Back | Close

Full Screen / Esc

Printer-friendly Version

Interactive Discussion

circulation, it can lead to a rather efficient transport of biomass burning products over the Indian sub-continent and Tibetan plateau. In particular, the modelling investigation conducted by Verma et al. (2008) for the period January–March 1999, showed that BC emitted by open fires in north Africa – west Asia may contribute up to 30–40% of the 550 nm – AOD over the Himalayan region. The rather high BC levels (101 ng m^{-3} and 91 ng m^{-3}, respectively) observed at NCO-P under SW-AP and W-NA circulation can support this possibility. In agreement with investigations during INDOEX (Rasch et al., 2001; Verma, 2006) and results provided by Koch et al. (2007), it suggests that a transport channel from western Asia and Africa towards southern Asia and the Himalayas may contribute to explaining the high night-time BC levels observed during the pre-monsoon period at NCO-P.

During the pre-monsoon season, a not negligible fraction of the time (24%) was also affected by REG circulation, characterised by the direct uplift of regional air-masses to NCO-P (Fig. 10). High values of BC, O$_3$, and coarse particle concentrations (96 ng m^{-3}, 61 ppbv and 0.16 cm^{-3}, respectively) were also observed during the night-time circulation (Table 3). From the LAGRANTO back-trajectory analysis, it was deduced that air-mass uplift by synoptic-scale processes could also play an appreciable role in transporting pollutants and mineral dust from the Asian Brown Cloud regions to NCO-P and the southern Himalayas. For instance, as shown by Bhowmik et al. (2008) and Kiguchi and Matsumoto (2005), the interaction of Himalayan orography with low level circulation induced by westerly-disturbance over northern India, or through passages in the upper troposphere moving eastward along the southern edge of the Tibetan Plateau, may represent some of the synoptic-scale processes favouring this air-mass uplift during the pre-monsoon period.

5 Conclusion

Starting March 2006, continuous observations of atmospheric composition were carried out at the Nepal Climate Observatory – Pyramid (NCO-P), the highest WMO –

Atmospheric Brown Clouds in the Himalayas: first two years of observations

P. Bonasoni et al.

Full Screen / Esc

Printer-friendly Version

Interactive Discussion

GAW Station (5079 m a.s.l.) not far from the Everest Base Camp. These activities were performed in the framework of SHARE (Station at High Altitude for Environmental research) Ev-K^2-CNR and ABC (Atmospheric Brown Clouds) UNEP projects. In the present paper, the first two years (March 2006–February 2008) of atmospheric compound observations are introduced and discussed, in relation to seasonal weather conditions and regional and synoptic circulations. Moreover, the possible connections between the atmospheric observations at the NCO-P and the wide-scale accumulation of pollutants and mineral dust over South Asia during pre-monsoon, i.e. Atmospheric Brown Cloud, have been also investigated. Brown Cloud composition includes aerosols such as black carbon, soil dust coarse particles, as well as pollutant gases such as ozone: the seasonal and diurnal behaviours of these compounds at NCO-P, as well as their variability, have been analyzed and studied in this work, while the companion papers of this special issue cover other aspects of NCO-P observational activities (Decesari et al., 2009; Gobbi et al., 2010; Cristofanelli et al., 2010; Marinoni et al., 2010; Duchi et al., 2010; Sellegri et al., 2010; Marcq et al., 2010). In South Asia, pollutants present near the surface are transported vertically and horizontally by atmospheric winds, attaining an extension of thousands of kilometres and thickness up to 4 km (Ramanathan et al., 2008). This thick haze layer transported from South Asia and Indo-Gangetic Plains towards the Himalayas can be vented along the mountain valleys, reaching NCO-P, particularly during the pre-monsoon season when the highest seasonal values of BC, O_3 and coarse particles were registered: 316.9 ng m^{-3}, 60.9 ppbv, 0.37 cm^{-3}, respectively. The lowest concentrations occurred during the monsoon for BC and O_3 (49.6 ng m^{-3} and 33.6 ppbv, respectively), and the post-monsoon period for coarse particle (0.07 cm^{-3}), showing a clear seasonal variation of atmospheric compounds at NCO-P, with mean 2-year values of BC, O_3 and coarse particle numbers of 160 ng m^{-3}, 49 ppbv and 0.25 cm^{-3}, respectively.

The analysis of meteorological parameters and 5-days LAGRANTO back-trajectories showed that the atmospheric seasonal conditions at NCO-P are influenced by both the local mountain wind system and the large-scale Asian monsoon circulation. On

the synoptic scale, a westerly circulation prevails from October to May, while wet air-masses from South Asia are more frequently advected to the NCO-P during the summer monsoon.

Pollution events (high values of BC and O_3) related with long-range transport were observed at the NCO-P rather frequently during pre-monsoon, while only a few cases were registered during the monsoon onset periods (e.g. during June 2006 and May 2007). During the pre-monsoon season, events of pollution coming from South-Asia and Indo-Gangetic plain (Gobbi et al., 2010) with AOD values (at 500 nm) greater than 0.10 were observed at NCO-P, while mean values below 0.05 generally characterise typical remote high altitude areas (Saha et al., 2005). In addition to anthropogenic pollution, natural phenomena (e.g. stratospheric intrusions and dust transports) acting on the synoptic scales can also affect the atmospheric properties at NCO-P. As shown by Cristofanelli et al. (2010), 14.1% of analysed days were found to be affected by stratospheric intrusions, resulting in an average 27.1% (+13 ppbv) ozone increase and low BC levels (average value, 70 ng m^{-3}) as compared to periods not affected by such events. The 23 multiday episodes of mineral dust transport on the synoptic scale observed at NCO-P (Duchi et al., 2010) could significantly affect the coarse particle concentrations that accounted for about half the PM_{10} mass (Marinoni et al., 2010; Decesari et al., 2010). Such high concentrations of mineral dust, BC and O_3 at high altitudes can affect solar radiation absorption at the surface and in the atmosphere, thus influencing the regional climate and biogeochemical cycle.

The influence that synoptic-scale transport could have in determining O_3, BC and coarse aerosol concentrations during the pre-monsoon period, were analysed as a function of night-time air-mass back-trajectory clusters. For the considered compounds, the highest median values (68 ppbv, 124 ng m^{-3}, 0.44 cm^{-3}, respectively) related to Westerly-Middle East (W-ME) circulation, affecting the measurement site for 19% of nigh-time observations. Thus, even if during this season 26% of W-ME air-masses were probably influenced by air-mass transport from the stratosphere (Cristofanelli et al., 2010), it was likely that the remaining 74% of W-ME air masses favoured

the transport of high concentration of aerosol and ozone from the polluted Arabian, and Persian Gulf regions, and Indian subcontinent to NCO-P, significantly affecting the behaviour of these atmospheric compounds. Within the present framework, as also specified by Decesari et al. (2010) and Duchi et al. (2010), transport from arid source areas in the Middle East, Central Asia and South-West Asia may represent an important source of the coarse aerosols at NCO-P. However, the average BC seasonal values registered during the pre-monsoon season ($317\,\mathrm{ng\,m^{-3}}$) was considerably higher than the night-time W-ME median value ($124\,\mathrm{ng\,m^{-3}}$), which is supposed here to be representative of large scale circulation. In agreement with Decesari et al. (2010) and Marinoni et al. (2010), it is deduced that local and regional scale circulations represent synergic processes able to transport efficiently into the upper Himalayan troposphere large amounts of organic particulate matter, BC and inorganic ions, from the Indo-Gangetic Plain and the Nepalese Himalayan foothills where, favoured by the long dry season, the pollution from the Atmospheric Brown Cloud accumulates (Ramanathan et al., 2008, and references therein). In fact, as shown herein, on 90% of pre-monsoon days the valley wind represents a preferred channel for the transport of Brown Cloud polluted air-masses up to NCO-P and (probably) to higher altitudes, particularly during the pre-monsoon season. The interaction between polluted boundary layer air-masses rising along the valley slopes and clean "upper" tropospheric air-masses was also found to lead to frequent new particle formation events, as already shown by Venzac et al. (2008). The absorbing aerosols, like BC and mineral dust, transported to the high Himalayas can also affect the atmospheric regional radiative budget (Marcq et al., 2010) and, once deposited onto snow and glacier surfaces, also impact surface radiation budgets, probably accelerating cryosphere melting (Aoki et al., 2007; IPCC, 2007; Flanner et al., 2009).

In the framework of the ABC project, the results presented here contribute to filling the gap in knowledge concerning atmospheric composition over the high Himalayas, providing the basis for a better evaluation of the impact of anthropogenic and natural processes on radiative forcing and air-quality in this critical region (Ramanathan et

al., 2008). Future implementation of the observational capacities at the NCO-P GAW station (starting with continuous monitoring of CO, NO_x, CO_2, ...) will allow to better define the trend of atmospheric composition and the ABC hotspots characterizing the high Himalayas and its glaciers. Therefore, it seems very important that the extension

5 of the ABC research activity is accompanied by suitable policies at the local government and institutional levels, aimed at promoting a sensitive reduction of soot particle emissions, based on the proposals of Ramanathan et al. (2009), in the context of the SURYA project, recently strengthened during COP15 in Copenhagen (EPA, 2009).

References

Agrawal, M., Auffhammer, M., Chopra, U. K., Emberson, L., Iyngararasan, M., Kalra, N., Ra-
20 mana, M. V., Ramanathan, V., Singh, A. K., and Vincent, J.: Impacts of Atmospheric Brown Clouds on Agriculture, Part II of Atmospheric Brown Clouds: Regional Assessment Report with Focus on Asia, Project Atmospheric Brown Cloud, UNEP, Nairobi, Kenya, 2008.

Anderson, T. L. and Ogren, J. A.: Determining Aerosol Radiative Properties Using the TSI 3563 Integrating Nephelometer, Aerosol Sci. Tech., 29(1), 57–69, 1998.

25 Aoki, T., Motoyoshi, H., Kodama, Y., Yasunari, T. J., and Sugiura, K.: Variations of the snow physical parameters and their effects on albedo in Sapporo, Japan, Ann. Glaciol., 46, 375–381, 2007.

Baudo, R., Schommer, B., Belotti, C., and Vuillermoz, E.: From Himalaya to Karakoram: the spreading of the project Ev-K^2-CNR, in: Mountains witnesses of global changes research

in the Himalaya and Karakoram; SHARE – Asia project, Developments in Earth Surface Processes, edited by: Baudo, R., Tartari, G., and Vuillermoz, E., Elsevier, Amsterdam, 10, 33–49, 2007.

Barnard, J. C. and Long, C. N.: A simple empirical equation to calculate cloud optical thickness using shortwave broadband measurements, J. Appl. Meteorol., 43, 1057–1066, 2004.

Barros, A. P. and Lang, T. J.: Monitoring the Monsoon in the Himalayas: Observations in Central Nepal, June 2001, Mon. Weather Rev., 131, 1408–1427, 2003.

Bertolani, L., Bollasina, M., and Tartari, G.: Recent biennial variability of meteorological features in the Eastern Highland Himalayas, Geophys. Res. Lett., 27, 2185–2188, 2000.

Bhowmik, S. K., Roy, S. S., and Kundu, P. K.: Analysis of large-scale conditions associated with convection over the Indian monsoon region, Int. J. Climatol., 28, 797–821, doi:10.1002/joc.1567, 2008.

Bhowmik, S. K., Roy, S. S., and Kundu, P. K.: Analysis of large-scale conditions associated with convection over the Indian monsoon region, Int. J. Climatol., 28, 797–821, 2008.

Böhmer, J.: General climatic controls and topoclimatic variations in Central and High Asia, BOREAS, 35, 279–294, 2006.

Bollasina, M., Bertolani, L., and Tartari, G.: Meteorological observations at high altitude in Khumbu Valley, Nepal Himalayas, 1994–1999, Bull. Glaciol. Res., 19, 1–11, 2002.

Bonasoni, P., Laj, P., Bonafè, U., Calzolari, F., Cristofanelli, P., Marinoni, A., Roccato, F., Facchini, M. C., Fuzzi, S., Gobbi, G. P., Pichon, J. M., Venzac, H., Sellegri, K., Villani, P., Maione, M., Arduini, J., Petzold, A., Sprenger, M., Verza, G. P., and Vuillermoz, E.: The ABC-Pyramid: a scientific laboratory at 5079 m a.s.l. for the study of atmospheric composition change and climate. in: Mountains witnesses of global changes research in the Himalaya and Karakoram; SHARE- Asia project, Developments in Earth Surface Processes, edited by: Baudo, R., Tartari, G., and Vuillermoz, E., Elsevier, Amsterdam, p. 67–73, 65, Chapter 10, 2007.

Bonasoni, P., Laj, P., Angelini, F., Arduini, J., Bonafè, U., Calzolari, F., Cristofanelli, P., Decesari, S., Facchini, M. C., Fuzzi, S., Gobbi, G. P., Maione, M., Marinoni, A., Petzold, A., Roccato, F., Reger, J. C., Sellegri, K., Sprenger, M., Venzac, H., Verza, G. P., Villani, P., and Vuillermoz, E.: The ABC-Pyramid Atmospheric Research Observatory in Himalayas for aerosol, ozone and halocarbon measurements, Sci. Total Environ., 391, 241–251, 2008.

Bond, T. C., Streets, D. G., Yarber, K. F., Nelson, S. M., Woo, J.-H., and Klimont, Z.: A technology based global inventory of black carbon and organic carbon emissions from combustion, J. Geophys. Res., 109, D14203, doi:10.1029/2003JD003697, 2004.

4862

Carrico, C. M., Bergin, M. H., Shrestha, A., Dibb, J. E., Gomes, L., and Harris, J. M.: The importance of carbon and mineral dust to seasonal aerosol properties in the Nepal Himalayas, Atmos. Environ., 37, 2811–2824, 2003.

Carnuth, W., Kempfer, U., and Trickl, T.: Highlights of the Tropospheric Lidar Studies at IFU within the TOR Project, Tellus B, 54, 163–185, 2002.

Chapman, S. and Lindzen, R. S.: Atmospheric Tides, D. Reidel, 200 pp, 1970.

Chou, M.-D. and Suarez, M. J.: An efficient thermal infrared radiation parameterization for use in general circulation models, NASA Tech. Memo. 104606, 3, 85 pp, 1994.

Cristofanelli, P., Marinoni, A., Arduini, J., Bonafè, U., Calzolari, F., Colombo, T., Decesari, S., Duchi, R., Facchini, M. C., Fierli, F., Finessi, E., Maione, M., Chiari, M., Calzolai, G., Messina, P., Orlandi, E., Roccato, F., and Bonasoni, P.: Significant variations of trace gas composition and aerosol properties at Mt. Cimone during air mass transport from North Africa – contributions from wildfire emissions and mineral dust, Atmos. Chem. Phys., 9, 4603–4619, 2009, http://www.atmos-chem-phys.net/9/4603/2009/.

Cristofanelli, P., Bracci, A., Sprenger, M., Marinoni, A., Bonafè, U., Calzolari, F., Duchi, R., Laj, P., Pichon, J. M., Roccato, F., Venzac, H., Vuillermoz, E., and Bonasoni, P.: Tropospheric ozone variations at the Nepal climate observatory – pyramid (Himalayas, 5079 m a.s.l.) and influence of stratospheric intrusion events, Atmos. Chem. Phys. Discuss., 10, 1483–1516, 2010, http://www.atmos-chem-phys-discuss.net/10/1483/2010/.

de Laat, A. T., Lelievedl, J., and Roelofs, G. J.: Source analysis of carbon monoxide pollution during INDOEX 1999, J. Geophys. Res., 106, 28481–28495, 2001.

Decesari, S., Facchini, M. C., Carbone, C., Giulianelli, L., Rinaldi, M., Finessi, E., Fuzzi, S., Marinoni, A., Cristofanelli, P., Duchi, R., Bonasoni, P., Vuillermoz, E., Cozic, J., Jaffrezo, J. L., and Laj, P.: Chemical composition of PM_{10} and PM_1 at the high-altitude Himalayan station Nepal Climate Observatory – Pyramid (NCO-P) (5079 m a.s.l.), Atmos. Chem. Phys. Discuss., 9, 25487–25522, 2009, http://www.atmos-chem-phys-discuss.net/9/25487/2009/.

Dorling, S. R., Davies, T. D., and Pierce, C. E.: Cluster-Analysis – a Technique for Estimating the Synoptic Meteorological Controls on Air and Precipitation Chemistry – Method and Applications, Atmos. Environ., Part a – General Topics, 26, 2575–2581, 1992.

Dubovik, O. and King, M. D.: A flexible inversion algorithm for retrieval of aerosol optical properties from sun and sky radiance measurements, J. Geophys. Res., 105, 20673–20696, 2000.

Duchi, R., Cristofanelli, P., Marinoni, A., Calzolari, F., Decesari, S., Laj, P., Sprenger, M., Vuillermoz, E., and Bonasoni, P., Mineral dust transport events at NCO-P (South Himalayas, 5079 m a.s.l.), Atmos. Chem. Phys. Discuss., in preparation, 2010.

EPA: Partnership for Clean Indoor Air Side Event, COP15, Copenhagen, 9 December 2009.

Flanner, M. G., Zender, C. S., Hess, P. G., Mahowald, N. M., Painter, T. H., Ramanathan, V., and Rasch, P. J.: Springtime warming and reduced snow cover from carbonaceous particles, Atmos. Chem. Phys., 9, 2481–2497, 2009,
http://www.atmos-chem-phys.net/9/2481/2009/.

Gautam, R., Liu, Z., Singh, R. P., and Hsu, N. C.: Two contrasting dust-dominant periods over India observed from MODIS and CALIPSO, Geophys. Res. Lett., 36, L06813, doi:10.1029/2008GL036967, 2009.

GAW report of the WMO meeting of experts on the quality assurance plan for the Global Atmospheric Watch (GAW), Garmisch-Partenkirchen, Germany, 26–30 March 1992.

Gobbi, G. P., Angelini, F., Bonasoni, P., Verza, G. P., Marinoni, A., and Barnaba, F.: Sunphotometry of the 2006–2007 aerosol optical/radiative properties at the Himalayan Nepal Climate Observatory Pyramid (5079 m a.s.l.), Atmos. Chem. Phys. Discuss., 10, 1193–1220, 2010,
http://www.atmos-chem-phys-discuss.net/10/1193/2010/.

Henne, S., Dommen, J., Neininger, B., Reimann, S., Staehelin, J., and Prévôt, A. S. H.: Influence of mountain venting in the Alps on the ozone chemistry of the lower free troposphere and the European pollution export, J. Geophys. Res., 110, D22307, doi:10.1029/2005JD005936, 2005.

Henne, S., Furger, M., Nyeki, S., Steinbacher, M., Neininger, B., de Wekker, S. F. J., Dommen, J., Spichtinger, N., Stohl, A., and Prévôt, A. S. H.: Quantification of topographic venting of boundary layer air to the free troposphere, Atmos. Chem. Phys., 4, 497–509, 2004,
http://www.atmos-chem-phys.net/4/497/2004/.

Henne, S., Klausen, J., Junkermann, W., Kariuki, J. M., Aseyo, J. O., and Buchmann, B.: Representativeness and climatology of carbon monoxide and ozone at the global GAW station Mt. Kenya in equatorial Africa, Atmos. Chem. Phys., 8, 3119–3139, 2008,
http://www.atmos-chem-phys.net/8/3119/2008/.

He, Y. J., Uno, I., Wang, Z. F., Pochanart, P., Li, J., and Akimoto, H.: Significant impact of the East Asia monsoon on ozone seasonal behavior in the boundary layer of Eastern China and the west Pacific region, Atmos. Chem. Phys., 8, 7543–7555, 2008,
http://www.atmos-chem-phys.net/8/7543/2008/.

Atmospheric Brown Clouds in the Himalayas: first two years of observations

P. Bonasoni et al.

Atmospheric Brown Clouds in the Himalayas: first two years of observations

P. Bonasoni et al.

Hindman, E. E. and Upadhyay, B. P.: Air pollution transport in the Himalayas of Nepal and Tibet during the 1995–1996 dry season, Atmos. Environ., 36, 727–739, doi:10.1016/S1352-2310(01)00495-2, 2002.

Holben, B. N., Eck, T. F., Slutsker, I., Tanré, D., Buis, J. P., Setzer, A., Vermote, E., Reagan, J. A., Kaufman, Y., Nakajima, T., Lavenu, F., Jankowiak, I., and Smirnov, A.: AERONET-A federated instrument network and data archive for aerosol characterization, Remote Sens. Environ., 66, 1–16, 1998.

Huebert, B. J., Bates, T., Russell, P. B., Shi, G., Kim, Y. J., Kawamura, K,. Carmichael, G., and Nakajima, T.: An overview of ACE-Asia: Strategies for quantifying the relationships between Asian aerosols and their climatic impacts, J. Geophys. Res., 108(D23), 8633, doi:10.1029/2003JD003550, 2003.

Kain, J. S.: The Kain-Fritsch convective parameterization: an update, J. Appl. Meteorol., 43, 170–181, 2004.

Kiguchi, M. and Matsumoto, J.: The Rainfall Phenomena during the pre-monsoon period over the Indo-China peninsula in the GAME-IOP year, 1998, J. Meteorol. Soc. Jap., 83, 89–106, 2005.

Klausen J., Zellweger, C., Buchmann, B., and Hofer, P.: Uncertainty and bias of surface ozone measurements at selected Global Atmosphere Watch sites, J. Geophys. Res., 108(D19), 4622, doi:10.1029/2003JD003710, 2003.

Koch, D., Bond, T. C., Streets, D., Unger, N., and van der Werf, G. R.: Global impacts of aerosols from particular source regions and sectors, J. Geophys. Res., 112, D02205, doi:10.1029/2005JD007024, 2007.

Krishnamurti, T. N. and Blame, H. N.: Oscillations of a monsoon system. Part. 1 Observational aspects, J. Atmos. Sci., 33, 1937–1954, 1976.

Lau, K.-M., Kim, M.-K., and Kim, K.-M.: Asian summer monsoon anomalies induced by aerosol direct forcing: the role of the Tibetan Plateau, Clim. Dynam., 26(7–8), 855–864, doi:10.1007/s00382-006-0114-z, 2006.

Lelieveld, J., Hoor, P., Jöckel, P., Pozzer, A., Hadjinicolaou, P., Cammas, J.-P., and Beirle, S.: Severe ozone air pollution in the Persian Gulf region, Atmos. Chem. Phys., 9, 1393–1406, 2009,
http://www.atmos-chem-phys.net/9/1393/2009/.

Liu, D., Wang, Z., Liu, Z., Winker, D., and Trepte, C.: A height resolved global view of dust aerosols from the first year CALIPSO lidar measurements, J. Geophys. Res., 113, D16214,

doi:10.1029/2007JD009776, 2008.

Lindzen, R. S. and Chapman, S.: Atmospheric tides., Space Sci. Rev., 10, 3–188, 1969.

Long C. N. and Ackerman, T. P.: Identification of clear skies from broadband pyranometer measurements and calculation of downwelling, shortwave cloud effects, J. Geophys. Res., 105(D12), 15609–15626, 2000.

Marcq, S., Laj, P., Villani, P., Roger, J. C., Sellegri, K., Bonasoni, P., Marinoni, A., Cristofanelli, P., Vuillermoz, E., Verza, G. P., and Bergin, M.: Aerosol Optical Properties and Radiative Forcing in the High Himalayas Based on Measurements at the Nepal Climate Observatory – Pyramid Site (5079 m a.s.l), Atmos. Chem. Phys. Discuss., in preparation, 2010.

Maione, M., Giostra, U., Arduini, J., et al.: Observations of climate active gases at two high mountain sites: a comparison between continental Europe and the Himalayan range, Atmos. Chem. Phys. Discuss., in preparation, 2010.

Marinoni, A., Bonasoni, P., Cristofanelli, P., Calzolari, F., Decesari, S., Sellegri, K., Vuillermoz, E., Verza, G. P., and Laj, P.: Aerosol mass and black carbon concentrations, two year-round observations at NCO-P (5079 m, Southern Himalayas), Atmos. Chem. Phys. Discuss., in preparation, 2010.

Marshall, F. S., Covert, D. S., and Charlson, R. J.: Relationship between asymmetry parameter and hemispheric backscatter ratio-implications for climate forcing by aerosols, Appl. Optics, 34, 6306–6311, 1995.

Mühle, J., Zahn, A., Brenninkmeijer, C. A. M., Gros, V., and Crutzen, P. J.: Air mass classi-fication during the INDOEX R/V RonaldBrown cruise using measurements of nonmethane hydrocarbons, CH4, CO2, CO, 14CO, and δ18O(CO), J. Geophys. Res., 107(D19), 8021, doi:10.1029/2001JD000730, 2002.

Naja, M., Lal, S., and Chand., D.: Diurnal and seasonal variabilities in surface ozone at a high altitude site Mt Abu (24.6° N, 72.7° E, 1680 m a.s.l.), Atmos. Environ., 37, 4205–4215, 2003.

Nessler, R., Weingartner, E., and Baltensperger, U.: Effect of humidity on aerosol light absorp-tion and its implications for extinction and the single scattering albedo illustrated for a site in the lower free troposphere, J. Aerosol Sci, 36, 958–972, 2005.

Novelli, P. C., Masarie, K. A., Lang, P. M., Hall, B. D., Myers, R. C., and Elkins, J. W.: Reanalysis of tropospheric CO trends: Effects of the 1997–1998 wildfires, J. Geophys. Res., 108(D15), 4464, doi:10.1029/2002JD003031, 2003.

Ohara, T., Akimoto, H., Kurokawa, J., Horii, N., Yamaji, K., Yan, X., and Hayasaka, T.: An Asian emission inventory of anthropogenic emission sources for the period 1980–2020, Atmos.

Atmospheric Brown Clouds in the Himalayas: first two years of observations

P. Bonasoni et al.

Chem. Phys., 7, 4419–4444, 2007,
http://www.atmos-chem-phys.net/7/4419/2007/.

Panday, A. K. and Prinn, R. G.: Diurnal cycle of air pollution in the Kathmandu Valley, Nepal:
Observations, J. Geophys. Res., 114, D09305, doi:10.1029/2008JD009777, 2009.

Petenko, I. V. and Argentini, S.: The annual behaviour of the semidiurnal and diurnal pressure
variations in East Antarctica, J. Appl. Meteorol., 41(11), 1093–1100, 2002.

Petzold, A., Kramer, H., and Schonlinner, M.: Continuous measurement of atmospheric black
carbon using a multi-angle absorption photometer, Environ. Sci. Pollut. R., 4, 78–82, 2002.

Phandis, M. J., Levy II, H., and Moxim, W. J.: On the evolution of pollution from South
and Southeast Asia during the winter spring monsoon, J. Geophys. Res., 107(D24), 4790,
doi:10.1029/2002JD002190, 2002.

Prasad, A. K. and Singh, R. P.: Changes in aerosol parameters during major dust storm events
(2001–2005) over the Indo-Gangetic Plains using AERONET and MODIS data, J. Geophys.
Res., 112, D09208, doi:10.1029/2006JD007778, 2007.

Prospero, J. M., Ginoux, P., Torres, O., Nicholson, S. E., and Gill, T. E.: Environmental char-
acterization of global sources of atmospheric soil dust identified with the NIMBUS 7 Total
Ozone Mapping Spectrometer (TOMS) absorbing aerosol product, Rev. Geophys., 40(1),
1002, doi:10.1029/2000RG000095, 2002.

Pudasainee, D., Sapkota, B., Shrestha, M. L., Kaga, A., Kondo, A., and Inoue, Y.: Ground
level ozone concentrations and its association with NOx and meteorological parameters in
Kathmandu valley, Nepal, Atmos. Environ., 40(40), 8081–8087, 2006.

Raman, S., Niyogi, D. D. S., Simpson, M., and Pelom, J.: Dynamics of the elevated land plume
over the Arabian Sea and the Northern Indian Ocean during the northeasterly monsoon
and during the Indian Ocean Experiment (INDOEX), Geophys. Res. Lett., 29(16), 1817,
doi:10.1029/2001GL014193, 2002.

Rajevan, M. and Ravedekar, J.: South Asia, in: State of Climate 2006, edited by: Arguez, A.,
Special supplement to BAMS, 88, 2007.

Rajevan, M., Rebadekar, J., and Zubair, L.: South Asia, in: State of Climate 2007, edited by:
Levinson, D. H. and Lawrimore, J. H., Special supplement to BAMS, 98, 2008.

Ramanathan, V. and Crutzen, P. J.: New Directions: Atmospheric Brown "Clouds", Atmos.
Environ., 37, 4033–4035, 2003.

Ramanathan, V., Li, F., Ramana, M. V., Praveen, P. S., Kim, D., Corrigan, C. E., Nguyen, H.,
Stone, E. A., Schauer, J. J., Carmichael, G. R., Adhikary, B., and Yoon, S. C.: Atmospheric

Title Page

Abstract | Introduction

Conclusions | References

Tables | Figures

◄◄ | ►►

◄ | ►

Back | Close

Full Screen / Esc

Printer-friendly Version

Interactive Discussion

brown clouds: Hemispherical and regional variations in long-range transport, absorption, and radiative forcing, J. Geophys. Res., 112, D22S21, doi:10.1029/2006JD008124, 2007.

Ramanathan, V., Agrawal, M., Akimoto, H., Auffhammer, M., Devotta, S., Emberson, L., Hasnain, S. I., Iyngararasan, M., Jayaraman, A., Lawrence, M., Nakajima, T., Oki, T., Rodhe, H., Ruchirawat, M., Tan, S. K., Vincent, J., Wang, J. Y., Yang, D., Zhang, Y. H., Autrup, H., Barregard, L., Bonasoni, P., Brauer, M., Brunekreef, B., Carmichael, G., Chung, C. E., Dahe, J., Feng, Y., Fuzzi, S., Gordon, T., Gosain, A. K., Htun, N., Kim, J., Mourato, S., Naeher, L., Navasumrit, P., Ostro, B., Panwar, T., Rahman, M. R., Ramana, M. V., Rupakheti, M., Settachan, D., Singh, A. K., Helen, G. St., Tan, P. V., Viet, P. H., Yinlong, J., Yoon, S. C., Chang, W. C., Wang, X., Zelikoff, J., and Zhu, A.: Atmospheric Brown Clouds: Regional Assessment Report with Focus on Asia, Published by the United Nations Environment Programme, Nairobi, Kenya, 2008.

Rasch, P. J., Collins, W. D., and Eaton, B. E.: Understanding the Indian Ocean Experiment (INDOEX) aerosol distributions with an aerosol assimilation, J. Geophys. Res., 106(D7), 7337–7355, 2001.

Rosenfeld, D., Lohmann, U., Raga, G. B., O'Dowd, C. D., Kulmala, M., Fuzzi, S., Reissel, A., and Andreae, M. O.: Flood or Drought: How Do Aerosols Affect Precipitation?, Science, 321, 1309–1313, doi:10.1126/science.1160606, 2008.

Scheele, M. P. and Siegmund, P. C.: Estimating errors in trajectory forecasts using ensemble predictions, J. Appl. Meteorol., 40, 1223–1232, 2001.

Saha, A., Pant, P., Dumka, U. C., Hegde, P., Srivastava, M. K., and Sagar, R.: Aerosol Characteristics at a high-altitude station Nainital during the ISRO-GBP Land Campaign-II, in: Proceedings of the SRO-GBP Land-Campaign-II meeting, Physical Research Laboratory, Ahmadabad, 1–2 March 2005.

Sellegri, K., Laj, P., Venzac, H., Picard, D., Villani, P., Bonasoni, P., Marinoni, A., Cristofanelli, P., and Vuillermoz, E.: Seasonal variation of aerosol size distribution based on long-term measurements at the high altitude Himalayan site of Nepal Climate Observatory-Pyramid (5079 m), Nepal, Atmos. Chem. Phys. Discuss., in preparation, 2010.

Schiemann, R., Lüthi, D., and Schär, C.: Seasonality and Interannual Variability of the Westerly Jet in the Tibetan Plateau Region, J. Climate, 22, 2940–2957, 2009.

Shrestha, R. M. and Malla, S.: Air pollution from energy use in a developing country city: The case study of Kathmandu valley, Nepal, Energy, 21, 785–794, 1996.

Shrestha, A. B., Wake, C. P., Dibb, J. E., Mayewski, P., and Whitlow, S.: Seasonal variations

Atmospheric Brown Clouds in the Himalayas: first two years of observations

P. Bonasoni et al.

Title Page

Abstract	Introduction
Conclusions	References
Tables	Figures

|◄ | ►|

◄ | ►

Back | Close

Full Screen / Esc

Printer-friendly Version

Interactive Discussion

in aerosol concentrations and compositions in the Nepal Himalaya, Atmos. Environ., 34, 3349–3363, 2000.

Skamarock, W. C., Klemp, J. B., Dudhia, J., Gill, D. O., Barker, D. M., Duda, G. M., Huang, X.-Y., Wang, W., and Powers, J. G.: A description of the Advanced Research WRF Version 3, Boulder, CO, NCAR, 113 pp., 2008.

Sudo, K. and Akimoto, H.: Global source attribution of tropospheric ozone: Long-range transport from various source regions, J. Geophys. Res., 112, D12302, doi:10.1029/2006JD007992, 2007.

Tarasova, O. A., Brenninkmeijer, C. A. M., Jöckel, P., Zvyagintsev, A. M., and Kuznetsov, G. I.: A climatology of surface ozone in the extra tropics: cluster analysis of observations and model results, Atmos. Chem. Phys., 7, 6099–6117, 2007, http://www.atmos-chem-phys.net/7/6099/2007/.

Ueno, K. and Pokhrel, A. P.: Intra-seasonal variation of surface air temperature in Nepal Himalayas, MAUSAM, 53, 281–288, 2002.

Ueno, K., Kayastha, R. B., Chitrakar, M. R., Bajracharya, O. R., Pokhrel, A. P., Fujinami, H., Kadota, T., Iida, H., Manandhar, D. P., Hattori, M., Yasunari, T., and Nakawo, M.: Meteorological observations during 1994–2000 at the Automatic Weather Station (GEN-AWS) in Khumbu region, Nepal Himalayas, B. Glacier Res., 18, 23–30, 2001.

Ueno, K., Toyotsu, K., Bertolani, L., Tartari, G.: Stepwise onset of Monsoon Weather Observed in the Nepal Himalayas, Mon. Weather Rev., 136(7), 2507–2522, 2008.

Venzac, H., Sellegri, K., Laj, P., Villani, P., Bonasoni, P., Marinoni, A., Cristofanelli, P., Calzolari, F., Fuzzi, S., Decesari, S., and Facchini, M. C., Vuillermoz, E., and Verza, G. P.: High frequency of new particle formation in the Himalayas, Proc. Natl. Acad. Sci. USA, 105(41), 15666–15671, 2008.

Verma, S., Boucher, O., Venkataraman, C., Reddy, M. S., Müller, D., Chazette, P., and Crouzille, B.: Aerosol lofting from sea breeze during the Indian Ocean Experiment, J. Geophys. Res., 111, D07208, doi:10.1029/2005JD005953, 2006.

Verma, S., Venkataraman, C., and Boucher, O.: Origin of surface and columnar Indian Ocean Experiment (INDOEX) aerosols using source- and region-tagged emissions transport in a general circulation model, J. Geophys. Res., 113, D24211, doi:10.1029/2007JD009538, 2008.

Villani, P., Picard, D., Michaud, V., Laj, P., and Wiedensohler, A.: Design and Validation of a Volatility Hygroscopic Tandem Differential Mobility Analyzer (VH-TDMA) to Characterize

Title Page

Abstract | Introduction

Conclusions | References

Tables | Figures

◄ | ►

◄ | ►

Back | Close

Full Screen / Esc

the Relationships Between the Thermal and Hygroscopic Properties of Atmospheric Aerosol Particles, Aerosol Sci. Technol., 42, 729–741, doi:10.1080/02786820802255668, 2008.

Wernli, H. and Davies, H.: A Lagrangian-based analysis of extratropical cyclones. Part I: The method and some applications, Q. J. Roy. Meteorol. Soc., 123, 467–489, 1997.

Wang, T., Wong, H. L. A., Tang, J., Ding, A., Wu, W. S., and Zhank, X. C.: On the origin of surface ozone and reactive nitrogen observed at a remote mountain site in the north-eastern Qinghai-Tibetan Plateau, western China, J. Geophys. Res., 111, D08303, doi:10.1029/2005JD006527, 2006.

Webster, P. J., Magaa, V. O., Palmer, T. M., Shukla, J., Tomas, R. A., Yanai, M., and Yasunari, T.: Monsoons: processes, predictability, and the prospect of prediction, J. Geophys. Res., 103, 14451–14510, 1998.

Wiedensohler, A.: An approximation of the bipolar charge distribution for particles in the submicron size range, J. Aerosol Sci., 19, 387–389, 1988.

Washington, R., Todd, M., Middleton, N., and Goudie, A.: Dust-storm source areas determined by the total ozone monitoring spectrometer and surface observations, Ann. Assoc. Am. Geogr., 93, 297–313, 2003.

Zellweger, C., Forrer, J., Hofer, P., Nyeki, S., Schwarzenbach, B., Weingartner, E., Ammann, M., and Baltensperger, U.: Partitioning of reactive nitrogen (NO_y) and dependence on meteorological conditions in the lower free troposphere, Atmos. Chem. Phys., 3, 779–796, 2003, http://www.atmos-chem-phys.net/3/779/2003/.

Table 1. Identification of seasonal transitions as a function of the local weather regime.

Year	Season	Start day–End day
2006	Pre-monsoon	1 March–20 May
	Monsoon	21 May–26 September
	Post-monsoon	27 September–20 November
2007	Winter	21 November 2006–31 January 2007
	Pre-monsoon	1 February–5 June
	Monsoon	6 June–12 October
	Post-monsoon	13 October–14 November
2008	Winter	15 November–18 February 2008

Table 2. Seasonal average (mean±standard deviation) and median values of O_3, BC and coarse particle number at NCO-P during the period March 2006–February 2008. Seasons are defined following Table 1, and mean values are calculated from the N available daily values (last number).

	Pre-monsoon	Monsoon	Post-monsoon	Winter
O_3 (ppbv)	60.9±8.4; 60.8, 200	38.9±9.6 36.8, 244	46.3±5.0 46.8, 86	51.2±5.4 51.2, 167
BC (ng m^{-3})	316.9±342.9 212.0, 205	49.6±60.9 30.6, 258	135.3±78.5 108.3, 89	118.4±80.9 98.3, 168
Coarse (cm^{-3})	0.37±0.37 0.25, 203	0.09±0.02 0.03, 225	0.07±0.05 0.05, 88	0.16±0.14 0.11, 107

Table 3. Cluster frequency (%) and surface O_3, BC and coarse particle number statistical analysis according to the different back-trajectory clusters: median, standard deviation and number of 3-h average data (in brackets). The conditional probability (%) of obtaining observations exceeding the seasonal 75th percentile is also reported. Bold characters denote the air-mass cluster characterised by the highest median value.

| | Air mass back-trajectory clusters for pre-monsoon night-time | | | | | | |
	SW-AP	SW-AS	SW-BG	W-NA	W-ME	W-EU	REG
Cluster frequency	8.9%	11.9%	–	29.8%	19.3%	6.2%	23.9%
O_3 (ppbv)	55/9 (26) 12%	61/11 (39) 31%	– –	58/7 (90) 10%	**68/8** (49) 42%	60/6 (23) 22%	61/9 (80) 29%
BC $(ng\,m^{-3})$	101/90 (26) 27%	74/87 (39) 21%	– –	91/100 (92) 23%	**124/95** (68) 34%	69/87 (24) 17%	96/85 (83) 22%
Coarse (cm^{-3})	0.07/0.14 (25) 12%	0.06/0.06 (37) 5%	– –	0.10/0.18 (84) 19%	**0.44/0.64** (64) 58%	0.11/0.11 (21) 19%	0.16/0.38 (61) 33%
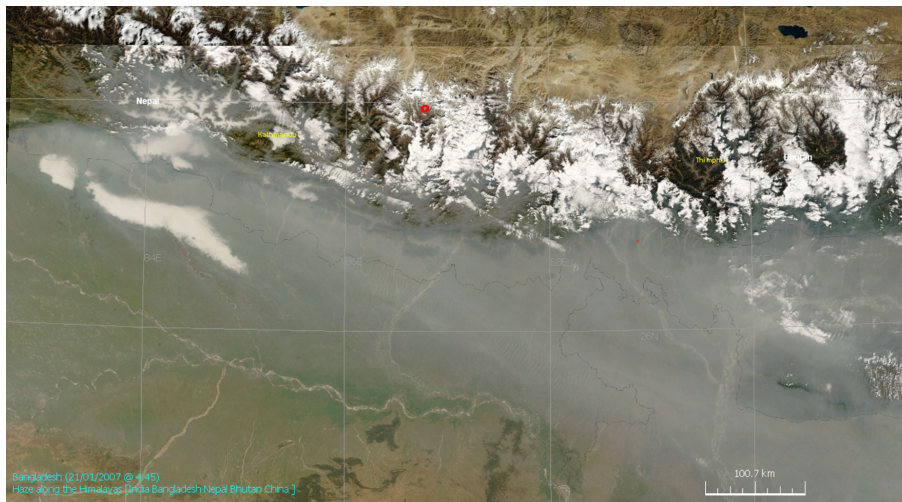
Fig. 1a. The Atmospheric Brown Cloud on southern slope of Himalayas (MODIS sensor on NASA Terra satellite, 21 January 2007) and location of the NCO-P (Nepal Climate Observatory – Pyramid, red point).

Fig. 1b. The Nepalese Khumbu valley (yellow line) and the NCO-P (red triangle). Modified by NASA World Wind, http://worldwind.arc.nasa.gov/.

ACPD

10, 4823–4885, 2010

Atmospheric Brown Clouds in the Himalayas: first two years of observations

P. Bonasoni et al.

Title Page

Abstract | Introduction

Conclusions | References

Tables | Figures

|◄ | ►|

◄ | ►

Back | Close

Full Screen / Esc

Printer-friendly Version

Interactive Discussion
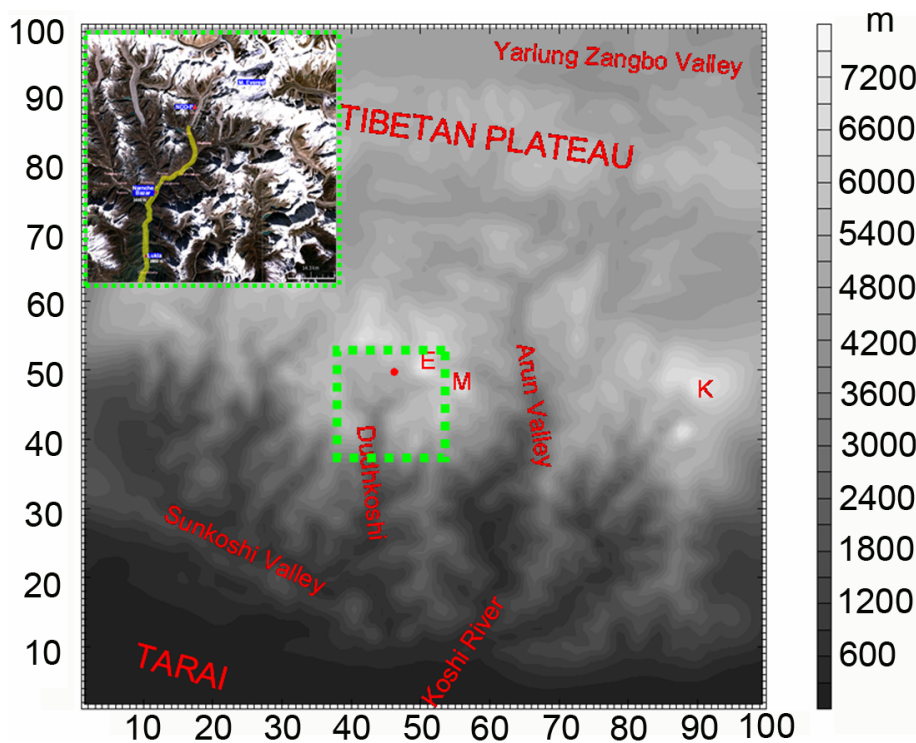
Fig. 2. Map of the domain of the third nest level in WRF simulations (surface elevation expressed in meters a.s.l., see coloured scale). NCO-P is marked by the red dot. Mountain peaks are denoted by single letters as follows: S=Shishapangma, E=Everest, M=Makalu, K=Kanchanjunga. For reference, the map of the valley region is also reported in the green box.

Atmospheric Brown Clouds in the Himalayas: first two years of observations

P. Bonasoni et al.

Title Page

Abstract | Introduction

Conclusions | References

Tables | Figures

|◄ | ►|

◄ | ►

Back | Close

Full Screen / Esc

Printer-friendly Version

Interactive Discussion
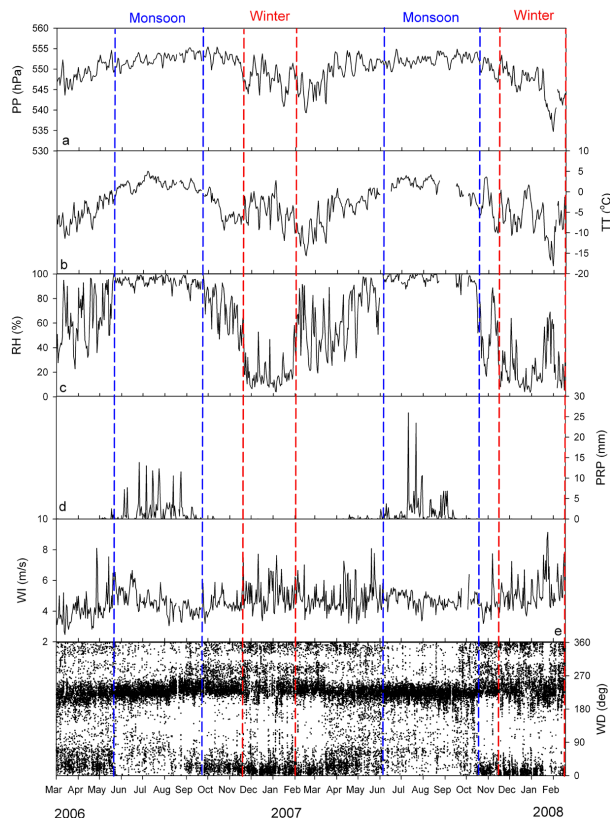
Fig. 3. Daily values of atmospheric pressure **(a)**, air-temperature **(b)**, relative humidity **(c)**, rain precipitation **(d)**, wind speed **(e)** and 30-min values of wind direction **(f)** at NCO-P from 1 March 2006 to 28 February 2008. Monsoon (blue) and winter (red) season onset and offset dates are represented by vertical lines.
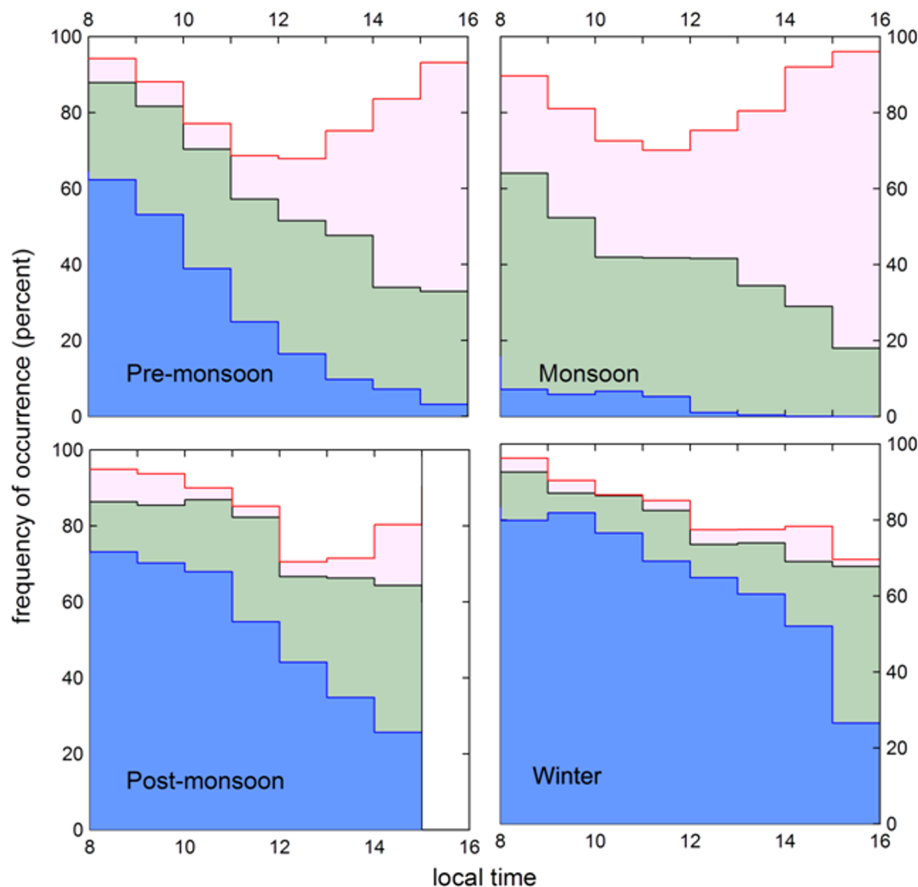
Fig. 4. Frequency of occurrence of clear skies (light blue), thin/moderate clouds (grey), thick clouds (pink), and scattered clouds (white) versus time of day for the different seasons, as derived from the CMP21 observations.

Title Page

Abstract	Introduction
Conclusions	References
Tables	Figures

◄◄   ►►

◄   ►

Back   Close

Full Screen / Esc

Printer-friendly Version

Interactive Discussion
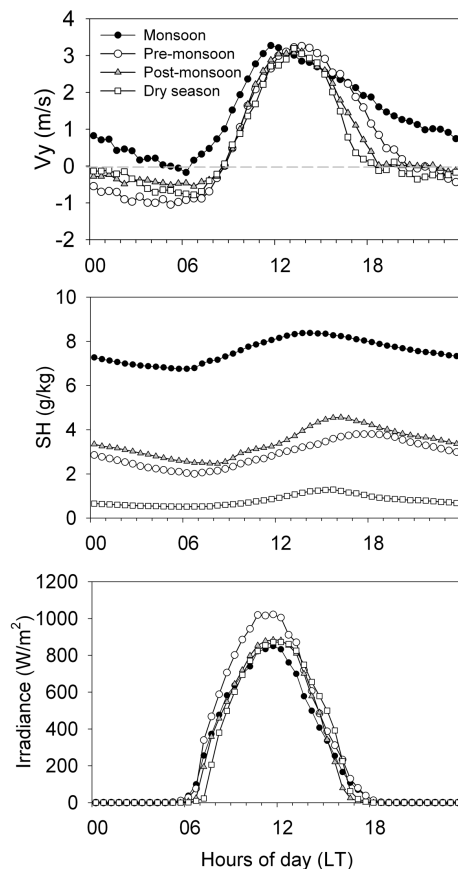
Fig. 5. Average seasonal diurnal variations of southerly wind component (Vy, upper plate), specific humidity (SH, middle plate) and solar irradiance (bottom plate) at NCO-P during the pre-monsoon (white circles), monsoon (black circles), post-monsoon (grey triangles) and winter (white squares) seasons.

Atmospheric Brown Clouds in the Himalayas: first two years of observations

P. Bonasoni et al.

Title Page

Abstract | Introduction

Conclusions | References

Tables | Figures

◄ | ►|

◄ | ►

Back | Close

Full Screen / Esc

Printer-friendly Version

Interactive Discussion
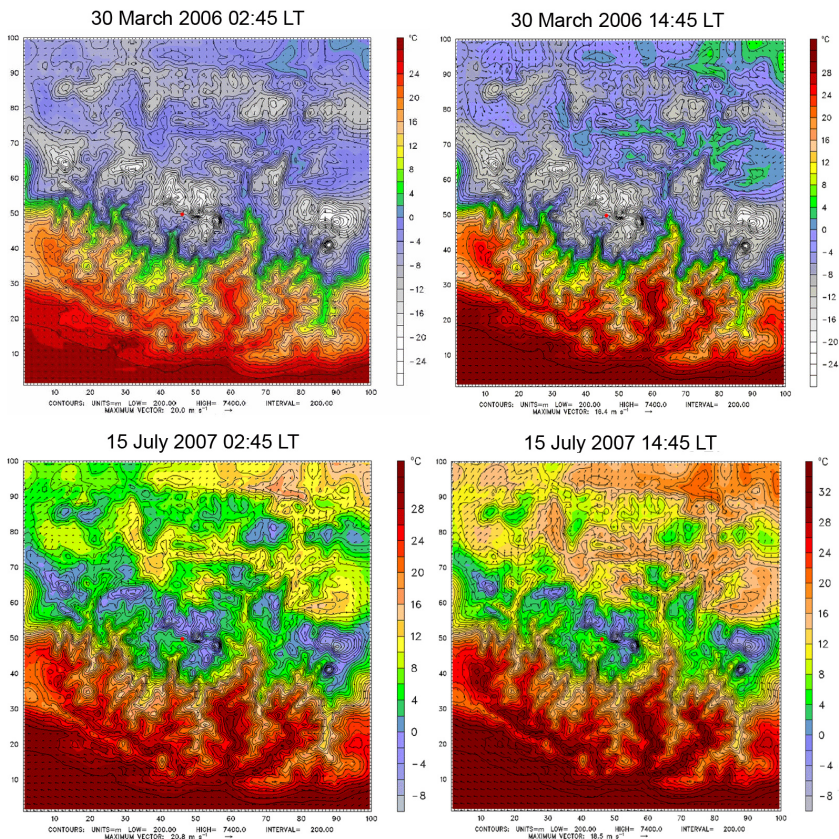
Fig. 6. 3 km resolution WRF model simulations in the region surrounding Mt. Everest during night-time (02:45 NST) and day-time (14:45 NST) for a specific pre-monsoon (30 March 2006) and monsoon day (15 July 2007). Temperature in the lowest model layer (150 m thick) is shown by the coloured field, while surface wind vectors are plotted in black. Terrain height is shown with a contour interval of 200 m. The red dot represents NCO-P location.
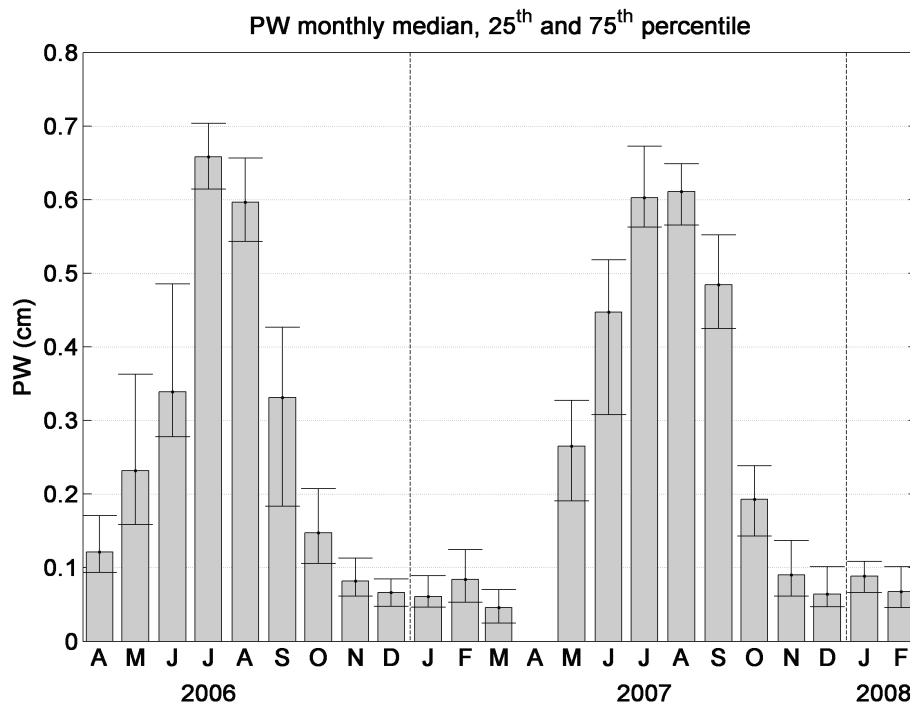
Fig. 7. Precipitable water monthly medians for the period April 2006–February 2008 at the EvK^2-CNR AERONET station at NCO-P. The error bars represent the 25th and 75th percentiles (e.g. Gobbi et al., 2010).
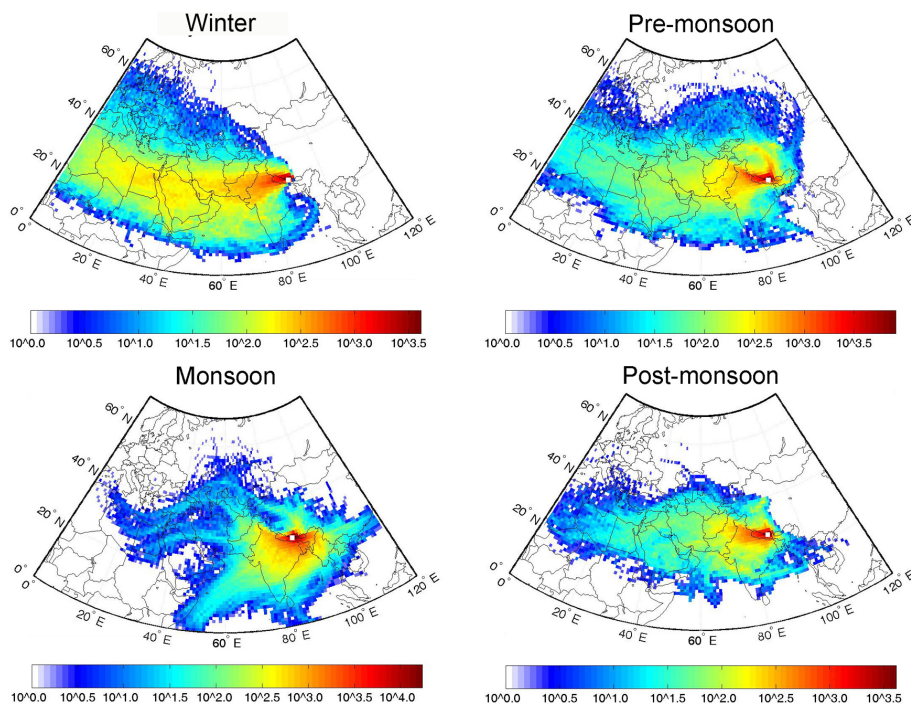
Fig. 8. Field concentrations (expressed as the logarithm of the number of back-trajectory points passing over a 1°×1° grid) of LAGRANTO back-trajectories for the seasons defined in Sect. 3.2.
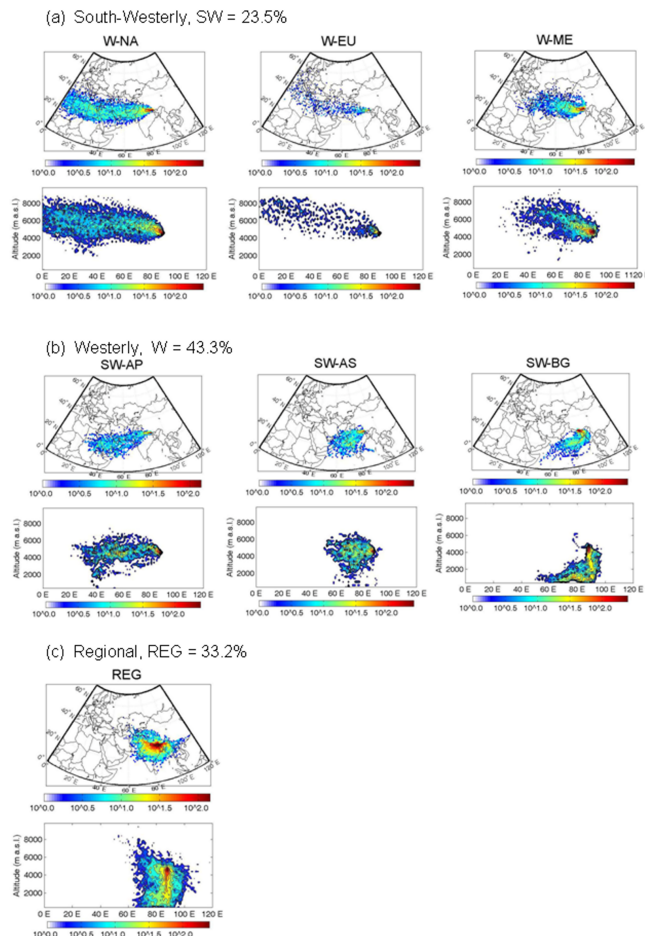
Fig. 9. Night-time three-dimensional back-trajectory cluster analysis at NCO-P for the period 1 March 2006–18 February 2008 (vertical cross section included).
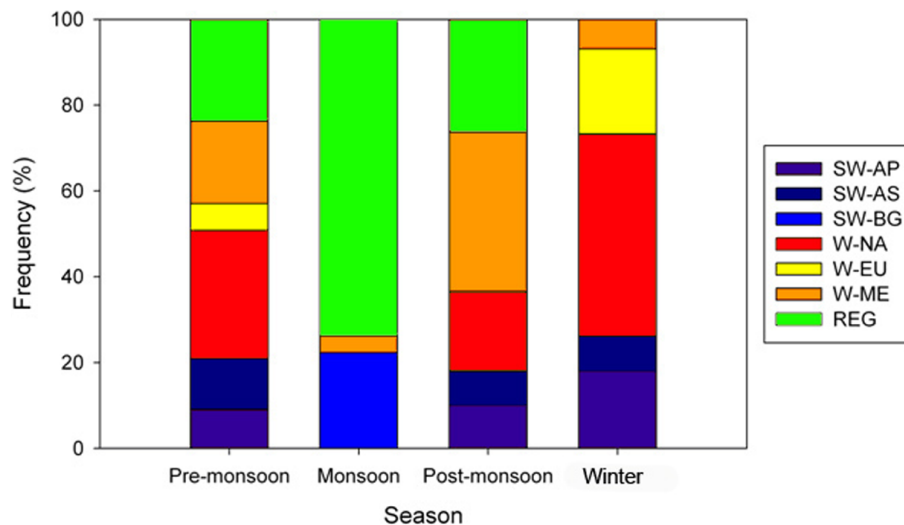
Fig. 10. Seasonal cluster frequencies at NCO-P for the period March 2006–February 2008: SW-AP (South Westerly – Arabian Peninsula), SW-AS (South Westerly – Arabian Sea), SW-BG (South Westerly – Bengal Gulf), W-NA (Westerly – North Africa), W-EU (Westerly – Europe), W-ME (Westerly – Middle East), REG (Regional).
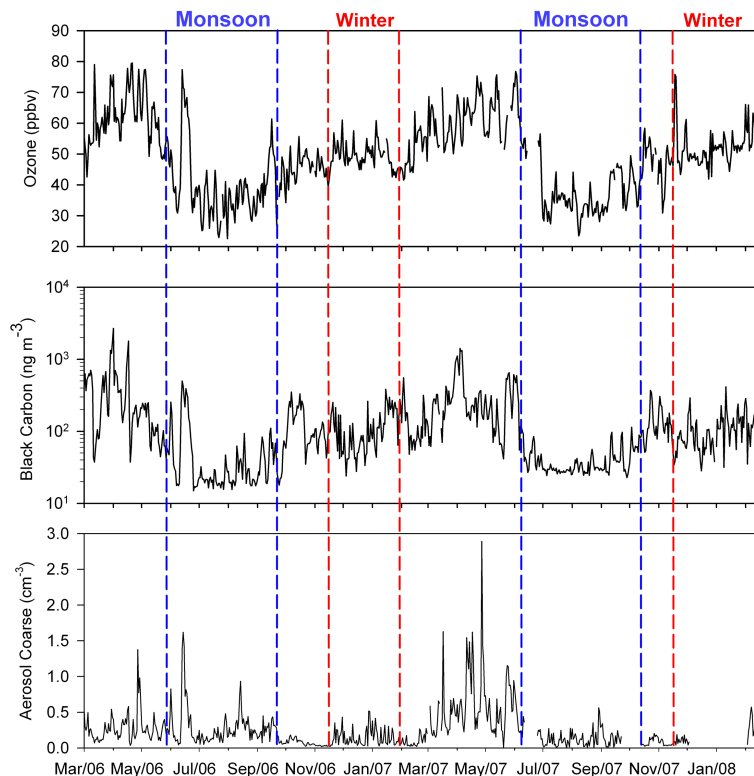
Fig. 11. Seasonal time series (daily averages) of surface O_3 (upper plate), BC (middle plate) and coarse particle number (button plate) at NCO-P from March 2006 to February 2008. Seasons (as defined in Table 1) are also reported: red – winter; light blue – monsoon. BC is reported by log-scale on y-axis.